SCIENTIFIC REPORTS

Mathematical Methods for the General Relativistic Two-body Problem

11 Aug 2025–15 Aug 2025

Organizing Committee

Alvin Chua

National University of Singapore

Soichiro Isoyama

National University of Singapore

Josh Mathews

National University of Singapore

Contents Page

ANALYTICAL MODELING OF GRAVITATIONAL WAVES: A RECENT VIEW ON THE POST-NEWTONIAN FRAMEWORK

LAURA BERNARD

Classification AMS 2020:

Keywords: general relativity, post-Newtonian formalism, perturbation theory, two-body problem

Next generation of gravitational wave detectors will have a tremendous sensibility, allowing many more gravitational wave detections over a very large frequency band. In particular, LISA, the future space-based detector, will be able to detect gravitational waves from supermassive black hole binaries and extreme/intermetdiate mass ratio inspirals. In order to learn the most from GW detections, one of the most prominent challenge lies in our ability to produce a bank of extremely accurate gravitational waveforms for all the expected sources.

To provide a consistent and unified description of the different phases of the coalescence of a binary system: inspiral, merger and ringdown (IMR), different methods are used. To describe the merger phase, where the strongest gravitational phenomena take place, solutions to the full nonlinear gravitational field equations are needed, which have been obtained with numerical relativity tools. On the other hand, the ringdown and inspiral stages of the coalescence can be described using perturbative techniques. For the former, BH perturbation theory is used to describe the relaxation phase, with the black hole quasi-normal modes playing a fundamental role. Finally, the inspiral phase is very accurately modeled with the multipolar post-Minkowskian – post-Newtonian (mPM-PN) formalism. It consists in a multipolar and weak field expansion combined with a series expansion in small velocities.

In this talk, I gave an overview of the mPM-PN framework in GR. In particular, I highlighted the similarities with more recent diagrammatic approaches, that all rely on a hierarchy on scales allowing to solve the two-body problem in successive region of space, and I insisted on the synergies and complementary between the different approaches.

Then, I presented the current state of the art, insisting on some recent results:

- the radiation-reaction at 4.5PN in the Burke-Thorne gauge;
- the gravitational flux and waveform at 4.5PN;
- some tail and memory contributions from EFT techniques;
- the finite-size effects amplitude modes at 4.5PN and the spinning amplitude modes at 3PN.

Finally, I concluded with some prospects in view of the next generation of gravitational wave detectors, insisting on:

- the interplay between PN and scattering amplitudes results;
- the interplay between PN and self-force and numerical relativity results to build full IMR waveforms;

- the importance of hereditary effects (tails, memory);
- the importance of improving current waveforms by including spin precession, high eccentricity and dynamical effects.

LUX, Observatoire de Paris-PSL, Meudon, France
Email address: laura.bernard@obspm.fr

DYNAMICAL TIDAL RESONANCES IN EMRIS

BÉATRICE BONGA

Classification AMS 2020:

Keywords:

Extreme-mass-ratio inspirals (EMRIs) are a key target for LISA, given that they are unique probes of the spacetime structure around the massive central black hole (BH) [1]. They will allow for extraordinarily precise tests of general relativity, since we will observe their intricate relativistic orbits over some $\sim 10^5$ orbits instead of $O(10)$ orbits in comparable-mass binaries observed by LIGO-Virgo-KAGRA. EMRIs are typically modeled as clean, isolated 2-body systems. Yet, in realistic galactic-center environments, other nearby stellar-mass objects can induce tidal resonances that leave an observable imprint on the gravitational waveform [2]. Without accounting for these resonant effects in our model, the utility of EMRIs as precision probes may be impeded. We may misattribute the effects to deviations from General Relativity or, worse, may not even be able to detect the EMRI. Conversely, if we can correctly model such tidal resonances, we unlock valuable information about the population of dark objects in the galactic core, otherwise difficult to access [3, 4].

Observational evidence has accumulated over the past years indicating the reality of such tidal perturbers with the observations of QPEs possibly describing the interaction of a stellar object with an accretion disk of a central massive BH [9, 10, 11, 12] and the discovery of new faint stars near SgrA* (such as S301 with a periapsis at only $\sim 260M_*$ with M_* the mass of SgrA*[8]). While EMRI rates with or without perturbers remain highly uncertain [15, 16], this highlights the importance of correctly incorporating tidal resonances in EMRI models.

To calculate the influence of a resonance on the waveform one needs to know when the resonance occurs and what the size of the effect is, which we will refer to as the 'jump'. A resonance occurs when the orbital frequencies of the EMRI with respect to Boyer-Lindquist time $\omega_r, \omega_\theta, \omega_\phi$ and of the tidal perturber become commensurate, i.e.,

$$n\,\omega_r + k\,\omega_\theta + m\,\omega_\phi + s\,\omega_{\rm td} = 0 \tag{0.1}$$

for integers n, k, m, s. The tidal perturber in principle also has three orbital frequencies, but since we take it to be at distances $\mathcal{O}(100M)$, its Keplerian frequency $\omega_{\rm td}$ is sufficient to describe its motion. In our earlier work [2, 3, 4], we assumed that the perturber is sufficiently far to be considered stationary during the resonance time (effectively setting $\omega_{\rm td}$ to zero in the resonance condition above). For such a stationary perturber there are a priori $9 \times 9 \times 5 = 405$ possible resonances with $|k|, |n| \leq 4$ and $|m| \leq 2$ (restricting to the leading-order, quadrupolar tidal deformation).[1] But considering symmetry properties and the condition that the resonance should occur in the LISA band — say, pragmatically,

[1]The perturbation is modeled by the leading order quadrupolar deformation of the central massive BH, which naturally restricts $|m| \leq 2$.

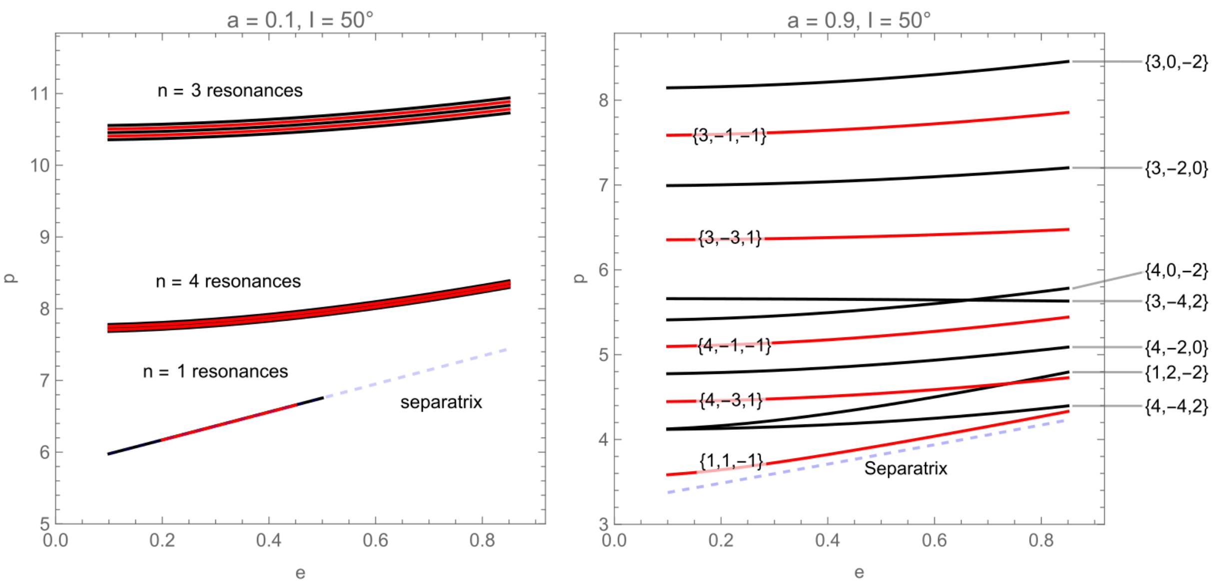

FIGURE 1. Resonance contours for a prograde orbit with inclination 50° in the eccentricity e - semilatus rectum p plane of the EMRI. The contour labels correspond to the resonance numbers $\{n, k, m\}$. The spin parameter of the central BH is set to $a = 0.1$ (left) and $a = 0.9$ (right). The blue dashed lines indicate the separatrix.

for a semi-latus rectum $< 100M$ — only 12 are allowable for a prograde orbit (and the same number for a retrograde orbit). The corresponding resonance contours are shown in Fig. 1. Resonances with the same n group together for small spin values of the central massive BH, while they diverge as the spin value increases (an effect somewhat reminiscent of Zeeman splitting). Both scenarios require extra care when implementing in Fast EMRI Waveforms (FEW) [17, 18, 19, 20]: for close resonances one has to make reasonably small steps to make sure one does not jump over a resonance contour, and when the resonances cross and overlap one has to account for both.

While for a typical EMRI evolution in the presence of a stationary tidal perturber, 12 resonances are possible, not all 12 resonances will be excited and produce observable imprints on the waveform. Whether a resonance is excited depends critically on the phase parameters with which the EMRI enters the resonance. Moreover, the impact on the waveform is also determined by the moment during the EMRI evolution it is excited. For instance, even if the instantaneous impact of the resonance is sizable, if the resonance occurs close to the separatrix, the impact on the waveform will be minimal as the resonance will only impact the final few orbits. Numerically evolving various EMRIs using the method of forced osculating orbital elements [21] seems to suggest that typically only 2-3 stationary resonances result in observable dephasing.[2]

Stationarity of the perturber is, however, not a good approximation: during a resonance for a perturber at realistic distances, the perturber typically completes 1-2

[2]Such a numerical evolution is computationally expensive (even when the radiation effects are modeled using 5PN fluxes as we did) and thus unsuitable for real-time waveform generation in data analysis pipelines.

orbital periods. Allowing for a dynamical perturber in principle also requires accounting for its possible eccentricity (known formation channels of tidal perturbers, such as two-body relaxation processes [13] and the Hills mechanism [14], suggest high eccentricities). Here, I will nevertheless assume that the perturber is in a circular orbit. This has the added benefit that we do not need to introduce any additional parameters compared to the stationary case.[3] The term $s\omega_{\rm td}$ in the resonance condition greatly enriches the allowed resonance structure: now there are more than 300 possible resonances in the LISA band (the exact number depends critically on the value of $\omega_{\rm td}$). Moreover, when the resonance occurs is no longer just determined by the EMRI evolution itself (i.e. $\omega_r, \omega_\theta, \omega_\phi$), but also depends on the additional parameter $\omega_{\rm td}$. A few exploratory numerical evolutions with the osculating elements code show some EMRI trajectories with 3 significant dynamic tidal resonances, but also some with as many as 17. This case is only just being explored and deserves further research. Key questions to address are: Which resonances dominate? Do we need to model all resonances for accurate phase modeling, or only the largest? How do self-force and tidal effects interact? Answering these questions and developing efficient implementations in FEW will be crucial for extracting maximal science from EMRI observations.

References

[1] L. Barack and C. Cutler, "LISA capture sources: Approximate waveforms, signal-to-noise ratios, and parameter estimation accuracy," *Phys. Rev. D* 69, 082005 (2004), arXiv:gr-qc/0310125.

[2] B. Bonga, H. Yang, and S. A. Hughes, "Tidal resonance in extreme mass-ratio inspirals," Phys. Rev. Lett. **123**, 101103 (2019), arXiv:1905.00030 [gr-qc].

[3] P. Gupta, B. Bonga, A. J. K. Chua, and T. Tanaka, "Importance of tidal resonances in extreme-mass-ratio inspirals," Phys. Rev. D **104**, 044056 (2021), arXiv:2104.03422 [gr-qc].

[4] P. Gupta, L. Speri, B. Bonga, A. J. K. Chua, and T. Tanaka, "Modeling transient resonances in extreme-mass-ratio inspirals," Phys. Rev. D **106**, 104001 (2022), arXiv:2205.04808 [gr-qc].

[5] B. Peters, "Tidal resonances in extreme mass ratio inspirals; A framework for studying stationary and dynamic tidal resonances," Master's thesis, Radboud University (2023).

[6] B. ten Brink, "Tidal resonances in extreme mass ratio inspirals; Investigating the behavior of static and dynamic tidal resonances," Master's thesis, Radboud University (2025).

[7] W. ten Haaf, "Dynamic Tidal Resonances in Extreme Mass Ratio Inspirals; Investigating the influence of the motion of the perturber," Master's thesis, Radboud University (2025).

[8] M. Sudan Bordoni, "Testing General Relativity at the Galactic Center with GRAVITY(+) and the ELT," Presentation at GR24-Amaldi16 (2025).

[9] G. Miniutti *et al.*, "Nine-hour X-ray quasi-periodic eruptions from a low-mass black hole galactic nucleus," Nature **573**, 381 (2019), arXiv:1909.04693 [astro-ph.HE].

[10] A. Franchini, M. Bonetti, A. Lupi, G. Miniutti, E. Bortolas, M. Giustini, M. Dotti, A. Sesana, R. Arcodia, and T. Ryu, "Quasi-periodic eruptions from impacts between the secondary and a rigidly precessing accretion disc in an extreme mass-ratio inspiral system," Astron. Astrophys. **675**, A100 (2023), arXiv:2304.00775 [astro-ph.HE].

[11] J. Chakraborty *et al.*, "Testing EMRI Models for Quasi-periodic Eruptions with 3.5 yr of Monitoring eRO-QPE1," Astrophys. J. **965**, 12 (2024), arXiv:2402.08722 [astro-ph.HE].

[12] C. Zhou, Z. Pan, N. Jiang, and W. Zhao, "Dynamical Measurement of Supermassive Black Hole Masses: QPE Timing Method," arXiv:2504.11078 [astro-ph.HE] (2025).

[3]The orbital speed of the perturber is completely determined by the ratio of the mass of the perturber to its distance from the central massive BH cubed, which we already needed to specify in the stationary setting to determine the strength of the tidal interaction.

[13] P. Amaro-Seoane, "Relativistic dynamics and extreme mass ratio inspirals," Living Rev. Rel. **21**, 4 (2018), arXiv:1205.5240 [astro-ph.CO].
[14] J. G. Hills, "Hyper-velocity and tidal stars from binaries disrupted by a massive Galactic black hole," Nature **331**, 687 (1988).
[15] S. Babak, J. Gair, A. Sesana, E. Barausse, C. F. Sopuerta, C. P. L. Berry, E. Berti, P. Amaro-Seoane, A. Petiteau, and A. Klein, "Science with the space-based interferometer LISA. V: Extreme mass-ratio inspirals," Phys. Rev. D **95**, 103012 (2017), arXiv:1703.09722 [gr-qc].
[16] Z. Pan, Z. Lyu, and H. Yang, "Wet extreme mass ratio inspirals may be more common for spaceborne gravitational wave detection," Phys. Rev. D **104**, 063007 (2021), arXiv:2104.01208 [astro-ph.HE].
[17] A. J. K. Chua, M. L. Katz, N. Warburton, and S. A. Hughes, "Rapid generation of fully relativistic extreme-mass-ratio-inspiral waveform templates for LISA data analysis," Phys. Rev. Lett. **126**, 051102 (2021), arXiv:2008.06071 [gr-qc].
[18] M. L. Katz, A. J. K. Chua, L. Speri, N. Warburton, and S. A. Hughes, "Fast extreme-mass-ratio-inspiral waveforms: New tools for millihertz gravitational-wave data analysis," Phys. Rev. D **104**, 064047 (2021), arXiv:2104.04582 [gr-qc].
[19] L. Speri, M. L. Katz, A. J. K. Chua, S. A. Hughes, N. Warburton, J. E. Thompson, C. E. A. Chapman-Bird, and J. R. Gair, "Fast and Fourier: Extreme Mass Ratio Inspiral Waveforms in the Frequency Domain," Front. Appl. Math. Stat. **9** (2024), arXiv:2307.12585 [gr-qc].
[20] C. E. A. Chapman-Bird *et al.*, "The Fast and the Frame-Dragging: Efficient waveforms for asymmetric-mass eccentric equatorial inspirals into rapidly-spinning black holes," arXiv:2506.09470 [gr-qc] (2025).
[21] J. R. Gair, E. E. Flanagan, S. Drasco, T. Hinderer, and S. Babak, "Forced motion near black holes," Phys. Rev. D **83**, 044037 (2011), arXiv:1012.5111 [gr-qc].

Institute for Mathematics, Astrophysics and Particle Physics, Radboud University, 6525 AJ Nijmegen, The Netherlands

Theoretical Sciences Visiting Program, Okinawa Institute of Science and Technology Graduate University, Onna, 904-0495, Japan
Email address: `bbonga@science.ru.nl`

THE NEXT STEPS: NOISE AND SYSTEMATIC BIAS IN EMRI INFERENCE

ALEXANDER (OLLIE) BURKE

Classification AMS 2020:

Keywords: Gravitational Waves, Extreme mass-ratio inspirals, Parameter Inference, Systematic Bias, Noise Modelling, Data Gaps.

1. Introduction

The Laser Interferometer Space Antenna (LISA) is a planned space-based gravitational wave observatory, set to launch in the 2030s [1]. One of LISA's key sources are extreme mass-ratio inspirals (EMRIs), systems where a stellar-mass compact object spirals into a massive black hole [2, 3]. EMRIs are expected to provide precise measurements of black hole properties and strong-field tests of general relativity [4–6]. However, accurate parameter inference from EMRI signals requires careful consideration of noise and systematic biases in the data analysis process. The purpose of my talk was to present recent advances in modelling noise and systematic biases in EMRI parameter inference, highlighting the implications for future LISA data analysis.

The true data stream for LISA can be parametrized as follows [7]:

(1.1)

$$d(t) = \underbrace{\sum_{j=1}^{J}\sum_{i=1}^{N_j} h_i^{(j)}(t;\boldsymbol{\theta}^{(j)},\boldsymbol{\lambda}_i^{(j)})}_{\text{Resolvable GW sources}} + \underbrace{\sum_{j=1}^{J}\Delta H_{\text{conf}}^{(j)}(t;\boldsymbol{\sigma})}_{\text{Confusion}} + \underbrace{\sum_{k=1}^{K}\sum_{p=1}^{N_p} G^{(k)}(t;\boldsymbol{\phi}^{(k)})_p}_{\text{Noise Transients}} + \underbrace{n_{\text{non stat}}(t)}_{\text{Non-stat noise}} + \underbrace{\ldots ?}_{\text{unknown}} .$$

Here, we see that the data stream is composed of multiple resolvable gravitational wave sources (e.g., EMRIs, massive black hole binaries, galactic binaries) [8–11], a confusion noise component arising from the unresolved sources [12–16], noise transients (glitches) [17–20], non-stationary noise components [19, 21, 22], and potentially other unknown contributions. Finally, due to the triangular configuration of the LISA craft, the equation above is one of three time-delay interferemometry (TDI) channels, each with their own noise characteristics and correlations [23]. Accurate modelling of the gravitational wave response and noise characteristics across these channels is essential for robust parameter inference. The purpose of this talk was to highlight how (1) overlapping signals, (2) inaccurate waveform models, and (3) data gaps (that impact the noise process) may potentially bias parameter estimation in the context of EMRIs.

2. Overlapping Signals

Focusing on N overlapping gravitational wave signals in the presence of stationary and Gaussian noise whilst neglecting confusion noise, glitches and un-modelled elements, the

Date: 15/08/2025.

data stream takes the form

$$d(t) = \sum_{i=0}^{N-1} h_i^{(i)}(t;\boldsymbol{\theta}^i) + n(t). \tag{2.1}$$

In the fully optimal case, where all N sources are fitted simultaneously, the log-likelihood is proportional to [24, 25]

$$\log\mathcal{L} \propto -\frac{1}{2}\left(d(t) - \sum_{i=0}^{N} h_m^{(i)}(\boldsymbol{\theta}^i)\middle| d - \sum_{i=0}^{N} h_m^{(i)}(\boldsymbol{\theta}^i)\right), \quad (a|b) = 4\Re\int_0^\infty \frac{\tilde{a}(f)\tilde{b}^*(f)}{S_n(f)}df, \tag{2.2}$$

where the notation $(\cdot|\cdot)$ represents the noise-weighted inner product. This approach uses a sum of model templates to describe the full data stream. However, in practice, fitting all sources simultaneously is computationally prohibitive. Instead, a sub-optimal approach is often employed where sources are fitted individually:

$$\log\mathcal{L} \propto -\frac{1}{2}\left(d(t) - h_m^{(k)}(\boldsymbol{\theta}^k)|d - h_m^{(k)}(\boldsymbol{\theta}^k)\right), \tag{2.3}$$

where only a single template is used to model the data. Here the data stream is given by

$$d(t) = \sum_{\substack{i=0\\ i\neq k}}^{N-1} h^{(i)}(t;\boldsymbol{\theta}^i) + n(t) \tag{2.4}$$

This sub-optimal approach introduces potential for bias when unresolved signals remain in the data [7].

This represents the "source confusion" – the sum of all other gravitational wave signals in the data stream that are not being fitted. The key insight is that potential biases are a result of unfitted templates. When signals overlap in frequency and time, the unfitted templates contaminate the parameter estimates of the source being analyzed, leading to systematic biases that can dominate over statistical uncertainties. During the talk, the author presented results from a study quantifying the impact of overlapping EMRIs and Massive Black Holes on parameter estimation. Three massive black hole signals and three EMRI waveforms were injected into Gaussian stationary noise. We performed parameter estimation using the software suite `Eryn` [26] and used state-of-the-art instrumental noise curves from the *LISA mission requirements* [27]. A "Global-fit", i.e., a simultaneous inference on the Massive black holes (treating EMRIs as confusion noise) were performed yielding statistically insignificant biases – all recovered parameters contained within the 1σ credible interval of the marginalised posterior distribution. Individual "local-fit" based parameter estimation schemes were performed on the EMRIs one at a time, in the presence of the residuals of the massive black holes after subtraction (and the other non-fitted EMRIs). Our results demonstrated that the biases on all EMRI parameters were statistically insignificant. This can be explained by the orthogonality of the EMRI waveforms in comparison to the massive black holes.

3. Inaccurate Waveform Models

The two-body problem in general relativity has no exact solution. Instead, approximate waveform models are used to describe gravitational wave signals [28, 29]. These models are derived using perturbative techniques, numerical relativity simulations, or phenomenological approaches. However, these approximations can introduce systematic biases in parameter estimation if the model does not accurately capture the true signal [30, 31]. For EMRIs, waveform models are built using black hole perturbation theory, where the small compact object is treated as a perturbation to the spacetime of the massive black hole. The accuracy of these models depends on the order of the perturbative expansion and the inclusion of various physical effects, such as self-force corrections and spin interactions. The purpose of this section of the talk was to highlight how inaccurate waveform models can bias parameter estimation for EMRIs and to present recent advances in quantifying and mitigating these biases.

Recent advances in waveform modeling have made available the first post-adiabatic waveforms for circular Schwarzschild orbits. The evolution equations for the orbital phase ϕ and frequency $\hat{\Omega}$ as a function of geodesic radius $\hat{r}$ in the post-adiabatic framework are given by [28]

$$\frac{d\phi}{dt} = \hat{\Omega}(\hat{r}), \tag{3.1}$$

$$\frac{d\hat{r}}{dt} = \underbrace{-\nu F_0^{\mathrm{SF}}(\hat{r})}_{\text{Adiabatic (0PA)}} - \underbrace{\hat{\nu}^2 F_1^{\mathrm{SF}}(\hat{r})}_{\text{Post-adiabatic (1PA)}} + \underbrace{\nu^2 F_1^{\mathrm{spin}}(\hat{r})}_{\text{Companion spin (1PA w/ spin)}} + \mathcal{O}(\nu^3), \tag{3.2}$$

where $\nu = M_1 M_2/(M_1 + M_2)^2 \ll 1$ is the symmetric mass-ratio. The first term represents the adiabatic (0PA) contribution, the second term is the post-adiabatic (1PA) correction, and the third term accounts for the companion spin at 1PA order. The dissipative energy flux at second order in the symmetric mass-ratio was computed in [29] with corresponding waveforms in [32], marking a breakthrough for gravitational self force providing, for the first time, second-order EMRI waveforms. Based on the work by the author in [30], we presented a study that investigated the impact of neglecting these 1PA terms on parameter estimation for EMRIs and intermediate mass-ratio inspirals (IMRIs) using Bayesian inference utilising the `FastEMRIWaveforms` framework [33]. The main findings were:

(1) Neglecting 1PA terms introduces significant biases for mass ratios $\epsilon \gtrsim 10^{-5}$ for quasi-circular orbits in Schwarzschild spacetime. These biases can be mitigated using resummed 3PN expressions at 1PA order.
(2) The secondary spin is strongly correlated with other intrinsic parameters and cannot be reliably constrained for $\epsilon \lesssim 10^{-5}$, highlighting the difficulty in measuring spin for true extreme mass-ratio systems.
(3) Models neglecting the 1PA spinning contribution may yield incorrectly enhanced precision statements on intrinsic parameters due to unaccounted correlations, particularly for mass ratios $\epsilon \gtrsim 10^{-3}$.

These results demonstrate that waveform model accuracy is critical for unbiased parameter estimation, particularly as LISA observations will span systems across a range of mass ratios where post-adiabatic corrections become essential.

4. Data Gaps and Noise Modelling

A critical yet often overlooked aspect of gravitational wave data analysis is the treatment of data gaps and the impact of noise mismodeling. Data gaps are unavoidable in LISA operations due to instrumental irregularities, scheduled maintenance, and data downlink periods [1]. These gaps disrupt the continuity of the data stream and violate the assumptions underlying the standard Whittle likelihood, which presumes stationary, continuous Gaussian noise [21, 22, 34].

Stationary noise implies that the auto-covariance matrix of the noise in the time-domain only depends on the time lag between two points. In the frequency domain, this leads to a diagonal noise covariance matrix [24]

$$\Sigma_n(f, f') = \langle \tilde{n}(f)\tilde{n}^*(f')\rangle = \frac{1}{2}S_n(f)\delta(f - f'), \tag{4.1}$$

where $\langle\cdot\rangle$ denotes an ensemble average, $\tilde{n}(f)$ is the Fourier transform of time series $n(t)$, the diract delta function δ enforces independence between frequency bins and $S_n(f)$ is the one-sided Power Spectral Density. One method to account for data gaps is to smoothly taper the data segments between gaps using window functions. Through this treatment, however, the noise covariance matrix in the frequency domain is no longer diagonal. Let $N(t) = w(t)n(t)$, for w a smooth taper function such that $w(t) = 0$ for $t \in T_{\text{gap}}$ and $w(t) = 1$ elsewhere, then

$$\Sigma_N(f, f') = \langle N(f)N^*(f')\rangle = \frac{1}{2}\int_{-\infty}^{\infty} \tilde{w}(f - u)\tilde{w}^*(f' - u)S_n(u)\,\mathrm{d}u\,, \tag{4.2}$$

rendering the Whittle-likelihood invalid. Equation (4.2) shows that frequency bins are now correlated and the likelihood must now take a different form. The purpose of this next (and final) section of the talk was to present preliminary results on an EMRI-like signal in gapped data, building on recent advances in the rigorous treatment of gapped data [21].

For this analysis, we considered a slowly evolving waveform template $h = A\sin(2\pi t(f_0 + \dot{f}_0 t)$ with parameters $\boldsymbol{\theta} = \{A, f_0, \dot{f}_0\}$ embedded in one-years worth of stationary Gaussian noise with a known PSD. This sinusoid could be thought of as a single harmonic of an EMRI. The data contained both long-duration gaps with period 14 days (mimicking antenna repointing procedures) and short-duration data gaps (100 second duration) occuring three times a day representing Point Ahead Angle Mechanism disturbances to the local Laser onboard the spacecraft. We considered two cases: (1) using rectangular window functions to model the gaps, and (2) using tapered window functions to smoothly transition between data segments. In both cases, we used the Fisher matrix procedure [25, 35–37] to quantify the bias arising from noise mismodelling in the presence of gaps. Our main findings were:

(1) The use of rectangular window functions leads to significant biases due to the excess leakage not accounted for in the Whittle-likelihood.
(2) Applying a smooth taper to the data segments significantly mitigates the bias. There is a trade off between bias and variance, as tapering reduces the effective SNR of the signal.

As demonstrated in [21], the inclusion of a tapering function improves statistical consistency of the gapped noise with respect to the non-gapped noise (and thus the Whittle-likelihood assumptions). We found that short-duration gaps may be problematic, even with tapering, due to the high frequency leakage introduced. Studies by the author are underway to implement the rigorous likelihood treatment for gapped data to assess the performance of various gap-mitigation strategies in the context of EMRI signals.

References

[1] Monica Colpi, Karsten Danzmann, Martin Hewitson, Kelly Holley-Bockelmann, Philippe Jetzer, et al. Lisa definition study report, 2024.

[2] Jonathan R Gair, Stanislav Babak, Alberto Sesana, Pau Amaro-Seoane, Enrico Barausse, Christopher PL Berry, Emanuele Berti, and Carlos Sopuerta. Prospects for observing extreme-mass-ratio inspirals with lisa. In *Journal of Physics: Conference Series*, volume 840, page 012021. IOP Publishing, 2017.

[3] Christopher P. L. Berry, Scott A. Hughes, Carlos F. Sopuerta, Alvin J. K. Chua, Anna Heffernan, Kelly Holley-Bockelmann, Deyan P. Mihaylov, M. Coleman Miller, and Alberto Sesana. The unique potential of extreme mass-ratio inspirals for gravitational-wave astronomy, 2019.

[4] Jonathan R Gair, Michele Vallisneri, Shane L Larson, and John G Baker. Testing general relativity with low-frequency, space-based gravitational-wave detectors. *Living Reviews in Relativity*, 16:1–109, 2013.

[5] Lorenzo Speri, Susanna Barsanti, Andrea Maselli, Thomas P Sotiriou, Niels Warburton, Maarten van de Meent, Alvin J K Chua, Ollie Burke, and Jonathan Gair. Probing fundamental physics with extreme mass ratio inspirals: a full Bayesian inference for scalar charge. *arXiv preprint arXiv:2406.07607*, 2024.

[6] Stanislav Babak, Jonathan R Gair, Alberto Sesana, Enrico Barausse, Carlos F Sopuerta, Christopher P L Berry, Emanuele Berti, Pau Amaro-Seoane, Antoine Petiteau, and Antoine Klein. Science with the space-based interferometer LISA. V: Extreme mass-ratio inspirals. *Physical Review D*, 95(10):103012, 2017.

[7] Andrea Antonelli, Ollie Burke, and Jonathan R Gair. Noisy neighbours: inference biases from overlapping gravitational-wave signals. *Monthly Notices of the Royal Astronomical Society*, 507(4):5069–5086, August 2021.

[8] Tyson B Littenberg and Neil J Cornish. Prototype global analysis of LISA data with multiple source types. *Physical Review D*, 107(6):063004, 2023.

[9] Michael L Katz, Nikolaos Karnesis, Natalia Korsakova, Jonathan R Gair, and Nikolaos Stergioulas. An efficient GPU-accelerated multi-source global fit pipeline for LISA data analysis. *Physical Review D*, 111(2):024060, 2024.

[10] Sylvain H Strub, Luigi Ferraioli, Chantal Schäfer, Aurélien Hees, and Eric Plagnol. Global analysis of LISA data with galactic binaries and massive black hole binaries. *arXiv preprint arXiv:2403.15318*, 2024.

[11] Shengrong Deng, Lorenzo Speri, Quentin Baghi, Sylvain Marsat, Stanislav Babak, and Michael L Katz. Modular global-fit pipeline for LISA data analysis. *arXiv preprint arXiv:2501.10277*, 2025.

[12] Matteo Bonetti and Alberto Sesana. Gravitational wave background from extreme mass ratio inspirals. *Physical Review D*, 102(10), November 2020.

[13] Federico Pozzoli, Stanislav Babak, Alberto Sesana, Matteo Bonetti, and Nikolaos Karnesis. Computation of stochastic background from extreme mass ratio inspiral populations for lisa, 2023.

[14] Manuel Piarulli, Riccardo Buscicchio, Federico Pozzoli, Ollie Burke, Matteo Bonetti, and Alberto Sesana. Test for lisa foreground gaussianity and stationarity: Extreme mass-ratio inspirals. *Physical Review D*, 111(10), May 2025.

[15] Davide Mancieri, Luca Broggi, Matteo Bonetti, and Alberto Sesana. Hanging on the cliff: Extreme mass ratio inspiral formation with local two-body relaxation and post-newtonian dynamics. *Astronomy amp; Astrophysics*, 694:A272, February 2025.

[16] Riccardo Buscicchio, Federico Pozzoli, Daniele Chirico, and Alberto Sesana. The first year of lisa galactic foreground, 2025.

[17] Martina Muratore, Jonathan Gair, Olaf Hartwig, Michael L. Katz, and Alexandre Toubiana. A pipeline for searching and fitting instrumental glitches in lisa data, 2025.

[18] Amin Boumerdassi, Matthew C. Edwards, Avi Vajpeyi, and Ollie Burke. First-time assessment of glitch-induced bias and uncertainty in inference of extreme mass ratio inspirals, 2025.

[19] LISA Consortium. Lisa pathfinder glitches. Available at: `https://lisa-simulation.pages.in2p3.fr/glitch/v1.2/lpf.html`. Accessed on 30 October 2025.

[20] Alice Spadaro, Riccardo Buscicchio, Daniele Vetrugno, Antoine Klein, Davide Gerosa, et al. Glitch systematics on the observation of massive black-hole binaries with lisa. *Physical Review D*, 108(12), December 2023.
[21] Ollie Burke, Sylvain Marsat, Jonathan R. Gair, and Michael L. Katz. Addressing data gaps and assessing noise mismodeling in LISA. *Phys. Rev. D*, 111(12):124053, 2025.
[22] Oliver Edy, Andrew Lundgren, and Laura K Nuttall. Issues of mismodeling gravitational-wave data for parameter estimation. *Physical Review D*, 103(12):124061, 2021.
[23] Massimo Tinto and Sanjeev V. Dhurandhar. Time-delay interferometry. *Living Reviews in Relativity*, 8(1), July 2005.
[24] P. Whittle. *Hypothesis Testing in Time Series Analysis*. Statistics / Uppsala universitet. Almqvist & Wiksells boktr., 1951.
[25] Lee S. Finn. Detection, measurement, and gravitational radiation. *Physical Review D*, 46(12):5236–5249, December 1992.
[26] Nikolaos Karnesis, Michael L. Katz, Natalia Korsakova, Jonathan R. Gair, and Nikolaos Stergioulas. Eryn : A multi-purpose sampler for Bayesian inference, 3 2023.
[27] Science requirement document: Esa-l3-est-sci-rs-001, 2018.
[28] Leor Barack and Adam Pound. Self-force and radiation reaction in general relativity. *Reports on Progress in Physics*, 82(1):016904, November 2018.
[29] Adam Pound and Barry Wardell. Black hole perturbation theory and gravitational self-force. *Handbook of Gravitational Wave Astronomy*, pages 1–119, 2022.
[30] Ollie Burke, Gabriel Andres Piovano, Niels Warburton, Philip Lynch, Lorenzo Speri, Chris Kavanagh, Barry Wardell, Adam Pound, Leanne Durkan, and Jeremy Miller. Accuracy requirements: Assessing the importance of first post-adiabatic terms for small-mass-ratio binaries, 2024.
[31] Hassan Khalvati, Philip Lynch, Ollie Burke, Lorenzo Speri, Maarten van de Meent, and Zachary Nasipak. Systematic errors in fast relativistic waveforms for extreme mass ratio inspirals, 2025.
[32] Barry Wardell, Adam Pound, Niels Warburton, Jeremy Miller, Leanne Durkan, and Alexandre Le Tiec. Gravitational Waveforms for Compact Binaries from Second-Order Self-Force Theory. *Phys. Rev. Lett.*, 130(24):241402, 2023.
[33] Michael L. Katz, Alvin J. K. Chua, Lorenzo Speri, Niels Warburton, and Scott A. Hughes. FastEMRIWaveforms: New tools for millihertz gravitational-wave data analysis, 4 2021.
[34] Colm Talbot, Eric Thrane, Sylvia Biscoveanu, and Rory Smith. Inference with finite time series: Observing the gravitational Universe through windows. *Phys. Rev. Res.*, 3(4):043049, 2021.
[35] Eanna E. Flanagan and Scott A. Hughes. Measuring gravitational waves from binary black hole coalescences: 2. The Waves' information and its extraction, with and without templates. *Phys. Rev. D*, 57:4566–4587, 1998.
[36] Mark Miller. Accuracy requirements for the calculation of gravitational waveforms from coalescing compact binaries in numerical relativity. *Phys. Rev. D*, 71:104016, May 2005.
[37] Curt Cutler and Michele Vallisneri. Lisa detections of massive black hole inspirals: Parameter extraction errors due to inaccurate template waveforms. *Phys. Rev. D*, 76:104018, Nov 2007.

School of Physics and Astronomy, University of Glasgow, Glasgow G12 8QQ, UK
Email address: ollie.burke@glasgow.ac.uk

FAST EMRI WAVEFORMS: FAST WAVEFORM GENERATION FOR ASYMMETRIC-MASS BINARIES

CHRISTIAN CHAPMAN-BIRD

Asymmetric-mass binary systems with mass ratios greater than 10, such as intermediate/extreme-mass-ratio inspirals (I/EMRIs), are information-rich gravitational-wave (GW) sources observable by both existing and future detectors, but their analysis requires accurate and efficient waveform models. Gravitational self-force techniques, combined with a two-timescale expansion, provide a viable route to achieving the required accuracy. In this talk, I will outline the current state of the Fast EMRI Waveforms (FEW) framework, which leverages this theoretical foundation to generate million-cycle EMRI waveforms in less than a second using interpolation of pre-computed data and hardware acceleration techniques. As an example of FEW in action, I will present a recently-developed model for fully-relativistic waveforms for eccentric equatorial inspirals into spinning central objects at adiabatic order, and discuss methods for quantifying the impact of systematics on the model accuracy. I will conclude with an overview of future directions for FEW development, including batched waveform generation and the incorporation of post-adiabatic effects.

UNIVERSITY OF BIRMINGHAM, UK
Email address: `c.chapman-bird@bham.ac.uk`

HYBRID POST-NEWTONIAN/SELF-FORCE INSPIRAL AND TRANSITION-TO-PLUNGE WAVEFORMS

GEOFFREY COMPÈRE

Keywords: Gravitational waves, gravitation, black holes, binary mergers, inspiral, post-Newtonian, self-force

Credits: This talk is based on [1, 2, 3] with contributions from L. Honet, A. Pound, J. Matthews, B. Wardell, G. Piovano, M. van de Meent and N. Warburton.

Since the first detection of a gravitational-wave (GW) signal 10 years ago (GW150914) [4], the LIGO-Virgo-KAGRA (LVK) collaboration has now seen more than a hundred binary coalescence events among their first three observing runs [5]. With the upcoming release of the fourth version of the Gravitational-Wave Transient Catalog (GWTC-4) and the fifth observing run planned for 2027 [6], many more GW events will soon be reported or discovered by ground-based detectors. Together with the improvement of detectors' sensitivity, this spurs GW modelers to provide fast and faithful waveform models for parameter estimation studies and tests of general relativity [7, 8, 9, 10, 11, 12].

In particular, one specific event from the third observing run, GW191219_163120, has been estimated to come from a binary with mass ratio $\sim$1:27. Such a high mass ratio lies beyond what current models are able to cover [5, 13] and points to one of the LVK observational science short-term R&D objectives: providing fast and accurate waveform models for asymmetric-mass-ratio binaries [14].

On the other side, future space-based detectors such as LISA will detect GW signals in the millihertz spectrum [15], allowing us to observe signals emitted by extreme-mass-ratio inspirals (EMRIs). The joint use of space-based detectors with future third-generation (3G) ground-based detectors such as the Einstein Telescope [16] will enable the observation of sources such as intermediate mass ratio coalescences (IMRACs) across multiple bandwidths [15]. Those intermediate systems with mass ratios typically ranging from $\sim$1:10^2 to $\sim$1:10^4 currently lack accurate waveform models and constitute a real GW modeling challenge for 3G detectors.

The waveform modeling technique that naturally leverages the existence of two disparate masses is the gravitational self-force (GSF or SF) program, where the Einstein field equations (EFEs) and the orbital motion of the secondary black hole are expanded in the binary's small mass ratio. Recent milestones in the self-force community have been, for example, the construction of a first-post-adiabatic (1PA)/second-order self-force (2GSF) waveform model for spinning binaries with a slowly spinning primary black hole and rapidly spinning, precessing secondary [17] and the development of a fast, data-analysis-ready adiabatic (0PA) model for eccentric equatorial binaries with a rapidly spinning primary in the `FEW` python package [18], leveraging the SF multiscale expansion framework [19, 20, 21, 22] and hardware acceleration [23] for rapidly generating waveforms.

1. Transition-to-plunge

These pieces of work focus primarily on the inspiral phase of the binary, which is expected to be sufficient for modeling EMRI signals. In contrast, IMRACs usually have a merger that occurs in the frequency band of ground-based detectors [15]. Moreover, recent results in second-order self-force [24, 13] show that self-force models can be remarkably precise even at more comparable mass ratios $\sim$1:10 [17, 25], and for such systems the merger can always represent a significant fraction of the signal-to-noise ratio (SNR). Those considerations make it important to extend the multiscale self-force framework beyond the innermost stable circular orbit (ISCO), where the inspiral motion of the binary breaks down.

A recent work by three of us [26] extensively derived the self-force framework for the transition-to-plunge (or simply "transition") motion of nonspinning, quasicircular binaries. This work extended the results of Refs. [27, 28, 29] by including a treatment of the Einstein field equations and waveform generation on top of the orbital dynamics, while also reformulating the transition in the phase-space approach [21, 22, 30] that underlies the multiscale expansion's accuracy [13] and efficiency.

In GSF theory, the merger-ringdown part of the waveform is generated by the secondary' final, approximately geodesic plunge into the primary after it transitions across the ISCO [31, 32]. Again, three of us recently showed how to formulate this regime in the phase-space approach of the multiscale expansion [33] (building on Refs. [34, 35]). This created a unified framework for inspiral, transition, and plunge that can be carried (in principle) to any order in the small mass ratio. In Ref. [36], two of us employed that framework to generate subleading-order merger-ringdown waveforms in a test case of modified gravity.

These developments have paved the way for building the first inspiral-merger-ringdown (IMR) model for quasicircular, nonspinning binaries beyond leading order in GSF theory [37, 38, 39, 40]. (See Refs. [41, 42, 43] for earlier such waveforms at leading order, following an iterative method initiated in Ref. [44] rather than a multiscale approach.)

With a first complete beyond-leading-order GSF IMR waveform model for nonspinning binaries at hand, we now aim to to include additional physical parameters. The work presented in this talk represents one of the intermediate steps towards including the effects of the primary black hole spin in the IMR waveform model presented in Ref. [37, 38, 39, 40]: we derive and implement second-post-leading transition-to-plunge (2PLT) waveforms using the phase-space formalism for non-eccentric equatorial motion of a Schwarzschild secondary black hole around a primary Kerr black hole. Moreover, we build a composite waveform model that smoothly interpolates between an adiabatic (0PA) model in the early inspiral and a 2PLT transition model when reaching the ISCO using a matched asymptotic expansions procedure. We address and solve issues already raised in Ref. [26] about the accuracy of such composite models due to early-time transition residuals in the dynamics.

2. Hybrid models

There has been substantial recent progress toward more faithful waveform models in much of the binary parameter space, but all these models have limitations in the high-$\mathring{q}$ regime [45]. In PN theory, waveforms have been pushed to 4.5PN beyond leading order [46, 47, 48]; however, PN rapidly loses accuracy at high $\mathring{q}$ because the number of orbital cycles in the strong-field regime scales linearly with $\mathring{q}$. Links between scattering binaries and gravitationally bound systems [49, 50, 51, 52, 53, 54, 55, 56] have also allowed PM scattering calculations to inform models of inspirals [57, 58, 59, 60, 61], but application of these ideas to asymmetric systems is still in a germinal stage [62, 63, 64, 65, 66, 67]. The SXS collaboration's catalog of NR waveforms now contains 4170 simulations, including 164 with mass ratios $\mathring{q} > 8$ [68, 69, 70], and work on the high-$\mathring{q}$ regime is ongoing [71, 72, 73]; however, NR is still currently limited to mass ratios $\lesssim 20$, and it is not feasible for NR to explore the whole high-$\mathring{q}$ parameter space (and effectively impossible to model EMRIs with NR) due to the quadratic scaling of NR runtime with $\mathring{q}$ [74].

In principle, the challenges of high-$\mathring{q}$ modeling are met by SF theory, in which the small, secondary object is treated as a source of perturbations on the spacetime of the larger, primary black hole, and the spacetime metric is consequently expanded in powers of the small mass ratio $\mathring{\varepsilon}$. This approach has reached recent milestones in both accuracy and efficiency. By combining a multiscale formulation of the Einstein field equations [19, 20, 75, 21, 22, 76] with GPU acceleration, the FastEMRIWaveforms (FEW) package [77, 23, 78, 18] can generate long, LISA-length waveforms in tens of milliseconds. At the same time, the most advanced SF models have proved highly accurate for all mass ratios $\mathring{q} \gtrsim 10$ [13, 25, 79]. However, current SF models remain severely limited in their coverage of the binary parameter space, particularly for spinning and precessing systems.

It is generally accepted that, in order to meet LISA requirements, it is necessary and sufficient to go to second order in the SF expansion of the EFEs [45, 80, 81]. This is motivated by the fact that the phase of the GW signal admits an expansion of the form [19, 21]

$$\varphi(t, \mathring{\varepsilon}) = \frac{1}{\mathring{\varepsilon}}\varphi_{(0)}(\mathring{\varepsilon}t) + \varphi_{(1)}(\mathring{\varepsilon}t) + \mathcal{O}(\mathring{\varepsilon}), \tag{2.1}$$

where the first term of the expansion is the adiabatic (0PA) phase and the second term is the first post-adiabatic (1PA) correction. The former depends on the dissipative piece of the first-order self-force (1SF), while the latter depends on the full first-order self-force as well as the dissipative piece of the second-order self-force (2SF) [19, 20, 21].

Currently, the only available 1PA model is restricted to the case of nonspinning, quasicircular inspirals [13]. 0PA models are available for generic binaries involving a spinning primary, but they are limited to weak fields and small eccentricities [82] or else to equatorial systems whose orbital angular momentum is aligned with the primary's spin axis [18]. 0PA models also fall short of the necessary accuracy requirements for EMRIs. For IMRIs and other less extreme binaries, which will be observable when the two bodies are at much larger separations, even a 1PA model loses accuracy [25].

A recent Bayesian analysis [83] confirmed that neglecting 1PA corrections introduces significant biases on the parameter estimation for EMRIs and IMRIs. However, it also showed that these biases can be mitigated or entirely eliminated by approximating the

1PA terms with PN data. This is the starting point of our work: *to combine SF and PN results to construct a model that accurately covers the whole range of mass ratios* $10 \lesssim \mathring{q} \lesssim 10^6$ *and particularly covers the spinning binaries for which there are no complete 1PA models*.

More concretely, we seek to build a hybridized SF+PN model that achieves the following:

(1) To model EMRIs with sufficient accuracy for LISA, the model should be "exact" (accurate to 6 or more digits [84]) in its 0PA information and should be as complete as possible in its 1PA information. Since 0PA effects [75, 85, 86, 87], first-order conservative self-force effects [88, 89], and all linear-in-secondary-spin effects [90, 91, 92, 93, 94, 22] can now be calculated in SF theory for generic orbital configurations around a spinning primary, completing a hybrid EMRI model for spinning binaries requires using a PN approximation to the missing second-order dissipative self-force effects.

(2) To be efficient enough for LISA data analysis and to dovetail with the prevailing EMRI modeling program, the model should take the multiscale form [21, 22] that is compatible with the FEW rapid waveform-generation software package [77, 23, 78, 18].

(3) To be sufficiently accurate for long signals that extend into the weak field, in the mass-asymmetric but non-EMRI regime $10^{-4} \lesssim \mathring{\varepsilon} \lesssim 0.1$ [18], the model must contain terms beyond 1PA order [25]. More generally, for the purpose of achieving high accuracy over the broadest possible range of signals, all available PN information should be included.

(4) Following the principle of parsimony, we also aspire to keep the model as conceptually simple as possible and built entirely from first principles, with no calibration to NR data.

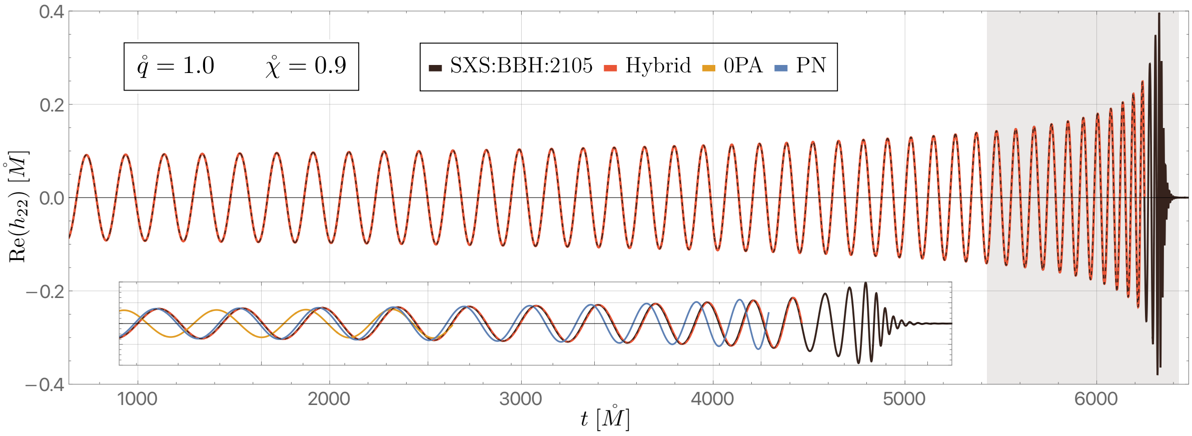

FIGURE 1. Self-force/post-Newtonian hybrid waveform (in red) and NR waveform SXS:BBH:2105 (in black) [95] for a quasicircular binary with primary spin $\mathring{\chi} = 0.9$ and mass ratio $\mathring{q} = 1$. The inset zooms in on the shaded gray region close to the merger. The hybrid model is described in the core of this article. We also display 0PA and 4PN waveforms for comparison (in orange and blue, respectively), aligned with the NR waveform at the same (early) reference time as the hybrid waveform.

In this talk, we develop a model achieving each of these objectives in the case of a nonspinning secondary object on a quasicircular orbit around a spinning primary black hole. Our model is restricted to the inspiral regime, but it could be extended to the merger-ringdown regime using the framework in Refs. [26, 33]. When applied for mass ratios $\mathring{q} \leq 15$, we find that our hybrid model matches NR inspiral waveforms far more accurately than either the 0PA or PN models taken individually. We find excellent numerical agreement with SXS simulations even at comparable mass ratios, as illustrated in Fig. 1 for an equal-mass, rapidly spinning binary.

Like the multiscale approach as a whole, our formulation (i) is modular, immediately improvable as PN and SF data advances, and (ii) will ultimately enable rapid generation of long waveforms for generic, eccentric, precessing binaries through seamless integration with the FEW package. We hence expect that our approach will provide accurate, efficient models of IMRIs and serve as accurate stand-ins for EMRI models until complete 1PA results are available.

In the Letter [1], we further extend our model to include additional SF information, and we provide a more thorough accuracy benchmarking against both NR and other models.

References

[1] L. Honet, J. Mathews, G. Compère, A. Pound, B. Wardell, G. A. Piovano, M. van de Meent, and N. Warburton, "Spin-aligned inspiral waveforms from self-force and post-Newtonian theory," 2510.16112.

[2] L. Honet, A. Pound, and G. Compère, "Hybrid waveform model for asymmetric spinning binaries: Self-force meets post-Newtonian theory," 2510.16114.

[3] L. Honet, L. Küchler, A. Pound, and G. Compère, "Transition-to-plunge self-force waveforms with a spinning primary," 2510.13958.

[4] **LIGO Scientific, Virgo** Collaboration, B. P. Abbott *et al.*, "Observation of Gravitational Waves from a Binary Black Hole Merger," *Phys. Rev. Lett.* **116** (2016), no. 6, 061102, 1602.03837.

[5] **KAGRA, LIGO Scientific, Virgo** Collaboration, B. P. Abbott *et al.*, "Gwtc-3: Compact binary coalescences observed by ligo and virgo during the second part of the third observing run," *Physical Review X* **13** (Dec., 2023).

[6] **LIGO Scientific** Collaboration, "Gravitational-wave candidate event database." https://gracedb.ligo.org. Accessed: 2025-02-04.

[7] A. Toubiana and J. R. Gair, "Indistinguishability criterion and estimating the presence of biases," 2024.

[8] E. E. Flanagan and S. A. Hughes, "Measuring gravitational waves from binary black hole coalescences. ii. the waves' information and its extraction, with and without templates," *Phys. Rev. D* **57** (Apr, 1998) 4566–4587.

[9] L. Lindblom, B. J. Owen, and D. A. Brown, "Model waveform accuracy standards for gravitational wave data analysis," *Phys. Rev. D* **78** (Dec, 2008) 124020.

[10] S. T. McWilliams, B. J. Kelly, and J. G. Baker, "Observing mergers of nonspinning black-hole binaries," *Phys. Rev. D* **82** (Jul, 2010) 024014.

[11] K. Chatziioannou, A. Klein, N. Yunes, and N. Cornish, "Constructing gravitational waves from generic spin-precessing compact binary inspirals," *Phys. Rev. D* **95** (May, 2017) 104004.

[12] M. Pürrer and C.-J. Haster, "Gravitational waveform accuracy requirements for future ground-based detectors," *Phys. Rev. Res.* **2** (May, 2020) 023151.

[13] B. Wardell, A. Pound, N. Warburton, J. Miller, L. Durkan, and A. Le Tiec, "Gravitational Waveforms for Compact Binaries from Second-Order Self-Force Theory," *Phys. Rev. Lett.* **130** (2023), no. 24, 241402, 2112.12265.

[14] **LVK** Collaboration, "The LSC-Virgo-KAGRA Observational Science White Paper (2024 Edition)," LIGO-T2300406-v1.
[15] **LISA** Collaboration, M. Colpi *et al.*, "LISA Definition Study Report." 2, 2024.
[16] **ET** Collaboration, M. Maggiore *et al.*, "Science Case for the Einstein Telescope," *JCAP* **03** (2020) 050, 1912.02622.
[17] J. Mathews, B. Wardell, A. Pound, and N. Warburton, "Post-adiabatic self-force waveforms: slowly spinning primary and precessing secondary," *to appear*.
[18] C. E. A. Chapman-Bird *et al.*, "The Fast and the Frame-Dragging: Efficient waveforms for asymmetric-mass eccentric equatorial inspirals into rapidly-spinning black holes." 6, 2025.
[19] T. Hinderer and E. E. Flanagan, "Two timescale analysis of extreme mass ratio inspirals in Kerr. I. Orbital Motion," *Phys. Rev.* **D78** (2008) 064028, 0805.3337.
[20] J. Miller and A. Pound, "Two-timescale evolution of extreme-mass-ratio inspirals: waveform generation scheme for quasicircular orbits in Schwarzschild spacetime," *Phys. Rev. D* **103** (2021), no. 6, 064048, 2006.11263.
[21] A. Pound and B. Wardell, "Black Hole Perturbation Theory and Gravitational Self-Force," in *Handbook of Gravitational Wave Astronomy*, p. 38. 2022. 2101.04592.
[22] J. Mathews and A. Pound, "Post-adiabatic waveform-generation framework for asymmetric precessing binaries." 1, 2025.
[23] M. L. Katz, A. J. K. Chua, L. Speri, N. Warburton, and S. A. Hughes, "Fast extreme-mass-ratio-inspiral waveforms: New tools for millihertz gravitational-wave data analysis," *Phys. Rev. D* **104** (2021), no. 6, 064047, 2104.04582.
[24] N. Warburton, A. Pound, B. Wardell, J. Miller, and L. Durkan, "Gravitational-Wave Energy Flux for Compact Binaries through Second Order in the Mass Ratio," *Phys. Rev. Lett.* **127** (2021), no. 15, 151102, 2107.01298.
[25] A. Albertini, A. Nagar, A. Pound, N. Warburton, B. Wardell, L. Durkan, and J. Miller, "Comparing second-order gravitational self-force, numerical relativity, and effective one body waveforms from inspiralling, quasicircular, and nonspinning black hole binaries," *Phys. Rev. D* **106** (2022), no. 8, 084061, 2208.01049.
[26] L. Küchler, G. Compère, L. Durkan, and A. Pound, "Self-force framework for transition-to-plunge waveforms," *SciPost Phys.* **17** (2024), no. 2, 056, 2405.00170.
[27] G. Compère and L. Küchler, "Self-consistent adiabatic inspiral and transition motion," *Phys. Rev. Lett.* **126** (2021), no. 24, 241106, 2102.12747.
[28] G. Compère and L. Küchler, "Erratum: Self-consistent adiabatic inspiral and transition motion [phys. rev. lett. 126, 241106 (2021)]," *Phys. Rev. Lett.* **128** (Jan, 2022) 029901.
[29] G. Compère and L. Küchler, "Asymptotically matched quasi-circular inspiral and transition-to-plunge in the small mass ratio expansion," *SciPost Phys.* **13** (2022), no. 2, 043, 2112.02114.
[30] J. Lewis, T. Kakehi, A. Pound, and T. Tanaka, "Post-adiabatic dynamics and waveform generation in self-force theory: an invariant pseudo-Hamiltonian framework," (7, 2025) 2507.08081.
[31] A. Ori and K. S. Thorne, "The Transition from inspiral to plunge for a compact body in a circular equatorial orbit around a massive, spinning black hole," *Phys. Rev.* **D62** (2000) 124022, gr-qc/0003032.
[32] A. Apte and S. A. Hughes, "Exciting black hole modes via misaligned coalescences: I. Inspiral, transition, and plunge trajectories using a generalized Ori-Thorne procedure," *Phys. Rev. D* **100** (2019), no. 8, 084031, 1901.05901.
[33] L. Küchler, G. Compère, and A. Pound, "Self-force framework for merger-ringdown waveforms," (6, 2025) 2506.02189.
[34] S. Hadar and B. Kol, "Post-ISCO Ringdown Amplitudes in Extreme Mass Ratio Inspiral," *Phys. Rev. D* **84** (2011) 044019, 0911.3899.
[35] A. Folacci and M. Ould El Hadj, "Multipolar gravitational waveforms and ringdowns generated during the plunge from the innermost stable circular orbit into a Schwarzschild black hole," *Phys. Rev. D* **98** (2018), no. 8, 084008, 1806.01577.

[36] A. Roy, L. Küchler, A. Pound, and R. Panosso Macedo, "Black hole mergers beyond general relativity: a self-force approach," (10, 2025) 2510.11793.
[37] L. Küchler, "Progress towards merger-ringdown waveforms from self-force theory." Talk given at 27th Capra Meeting on Radiation Reaction in General Relativity (National University of Singapore), https://www.caprameeting.org/capra-meetings/capra-27/abstracts, 2024.
[38] L. Küchler, "Self-force framework for transition-to-plunge waveforms." Talk given at 15th International LISA Symposium (University College Dublin), https://www.lisasymposium2024.ie/programme/, 2024.
[39] L. Küchler, "Self-force framework for transition-to-plunge waveforms." Talk given at Fundamental Physics Meets Waveforms with LISA Workshop (Max Planck Institute for Gravitational Physics, Potsdam), https://workshops.aei.mpg.de/fpmeetswavelisa/program/, 2024.
[40] L. Küchler, "Inspiral-merger-ringdown waveforms from gravitational self-force theory." Talk given at the 24th International Conference on General Relativity and Gravitation and the 16th Edoardo Amaldi Conference on Gravitational Waves (Glasgow, UK), https://iop.eventsair.com/gr24-amaldi16/conference-agenda, 2025.
[41] N. E. M. Rifat, S. E. Field, G. Khanna, and V. Varma, "Surrogate model for gravitational wave signals from comparable and large-mass-ratio black hole binaries," *Phys. Rev. D* **101** (2020), no. 8, 081502, 1910.10473.
[42] T. Islam, S. E. Field, S. A. Hughes, G. Khanna, V. Varma, M. Giesler, M. A. Scheel, L. E. Kidder, and H. P. Pfeiffer, "Surrogate model for gravitational wave signals from nonspinning, comparable-to large-mass-ratio black hole binaries built on black hole perturbation theory waveforms calibrated to numerical relativity," *Phys. Rev. D* **106** (2022), no. 10, 104025, 2204.01972.
[43] K. Rink, R. Bachhar, T. Islam, N. E. M. Rifat, K. Gonzalez-Quesada, S. E. Field, G. Khanna, S. A. Hughes, and V. Varma, "Gravitational wave surrogate model for spinning, intermediate mass ratio binaries based on perturbation theory and numerical relativity," *Phys. Rev. D* **110** (2024), no. 12, 124069, 2407.18319.
[44] P. A. Sundararajan, G. Khanna, and S. A. Hughes, "Towards adiabatic waveforms for inspiral into Kerr black holes. I. A New model of the source for the time domain perturbation equation," *Phys. Rev. D* **76** (2007) 104005, gr-qc/0703028.
[45] **LISA Consortium Waveform Working Group** Collaboration, N. Afshordi *et al.*, "Waveform Modelling for the Laser Interferometer Space Antenna." 11, 2023.
[46] T. Damour, P. Jaranowski, and G. Schäfer, "Nonlocal-in-time action for the fourth post-Newtonian conservative dynamics of two-body systems," *Phys. Rev. D* **89** (2014), no. 6, 064058, 1401.4548.
[47] L. Blanchet, G. Faye, Q. Henry, F. Larrouturou, and D. Trestini, "Gravitational-Wave Phasing of Quasicircular Compact Binary Systems to the Fourth-and-a-Half Post-Newtonian Order," *Phys. Rev. Lett.* **131** (2023), no. 12, 121402, 2304.11185.
[48] D. Trestini, "Schott term in the binding energy for compact binaries on circular orbits at fourth post-Newtonian order," *Phys. Rev. D* **112** (2025), no. 2, 024076, 2504.13245.
[49] T. Damour, "Gravitational scattering, post-Minkowskian approximation and Effective One-Body theory," *Phys. Rev.* **D94** (2016), no. 10, 104015, 1609.00354.
[50] T. Damour, "High-energy gravitational scattering and the general relativistic two-body problem," *Phys. Rev. D* **97** (2018), no. 4, 044038, 1710.10599.
[51] D. Bini, T. Damour, and A. Geralico, "Novel approach to binary dynamics: application to the fifth post-Newtonian level," *Phys. Rev. Lett.* **123** (2019), no. 23, 231104, 1909.02375.
[52] G. Kälin and R. A. Porto, "From Boundary Data to Bound States," *JHEP* **01** (2020) 072, 1910.03008.
[53] G. Kälin and R. A. Porto, "From boundary data to bound states. Part II. Scattering angle to dynamical invariants (with twist)," *JHEP* **02** (2020) 120, 1911.09130.
[54] G. Cho, G. Kälin, and R. A. Porto, "From boundary data to bound states. Part III. Radiative effects," *JHEP* **04** (2022) 154, 2112.03976. [Erratum: JHEP 07, 002 (2022)].
[55] M. V. S. Saketh, J. Vines, J. Steinhoff, and A. Buonanno, "Conservative and radiative dynamics in classical relativistic scattering and bound systems," *Phys. Rev. Res.* **4** (2022), no. 1, 013127, 2109.05994.

[56] T. Adamo, R. Gonzo, and A. Ilderton, "Gravitational bound waveforms from amplitudes," *JHEP* **05** (2024) 034, 2402.00124.
[57] A. Nagar, R. Gamba, P. Rettegno, V. Fantini, and S. Bernuzzi, "Effective-one-body waveform model for noncircularized, planar, coalescing black hole binaries: The importance of radiation reaction," *Phys. Rev. D* **110** (2024), no. 8, 084001, 2404.05288.
[58] A. Buonanno, G. Mogull, R. Patil, and L. Pompili, "Post-Minkowskian Theory Meets the Spinning Effective-One-Body Approach for Bound-Orbit Waveforms," *Phys. Rev. Lett.* **133** (2024), no. 21, 211402, 2405.19181.
[59] S. Albanesi, R. Gamba, S. Bernuzzi, J. Fontbuté, A. Gonzalez, and A. Nagar, "Effective-one-body modeling for generic compact binaries with arbitrary orbits," (3, 2025) 2503.14580.
[60] C. Dlapa, G. Kälin, Z. Liu, and R. A. Porto, "Local-in-Time Conservative Binary Dynamics at Fifth Post-Minkowskian and First Self-Force Orders," (6, 2025) 2506.20665.
[61] D. Akpinar, V. del Duca, and R. Gonzo, "Spinning self-force EFT: 1SF waveform recursion relation and Compton scattering," *Phys. Rev. D* **112** (2025), no. 8, 084014, 2504.02025.
[62] R. Gonzo and C. Shi, "Boundary to bound dictionary for generic Kerr orbits," *Phys. Rev. D* **108** (2023), no. 8, 084065, 2304.06066.
[63] L. Barack *et al.*, "Comparison of post-Minkowskian and self-force expansions: Scattering in a scalar charge toy model," *Phys. Rev. D* **108** (2023), no. 2, 024025, 2304.09200.
[64] C. Cheung, J. Parra-Martinez, I. Z. Rothstein, N. Shah, and J. Wilson-Gerow, "Gravitational scattering and beyond from extreme mass ratio effective field theory," *JHEP* **10** (2024) 005, 2406.14770.
[65] D. Kosmopoulos and M. P. Solon, "Gravitational self force from scattering amplitudes in curved space," *JHEP* **03** (2024) 125, 2308.15304.
[66] O. Long, C. Whittall, and L. Barack, "Black hole scattering near the transition to plunge: Self-force and resummation of post-Minkowskian theory," *Phys. Rev. D* **110** (2024), no. 4, 044039, 2406.08363.
[67] R. Gonzo, J. Lewis, and A. Pound, "First Law of Binary Black Hole Scattering," *Phys. Rev. Lett.* **135** (2025), no. 13, 131401, 2409.03437.
[68] "Sxs catalog." "data.black-holes.org".
[69] M. Boyle and M. Scheel, "The sxs package." 2024.0.18, https://www.black-holes.org.
[70] M. A. Scheel, M. Boyle, K. Mitman, N. Deppe, L. C. Stein, C. Armaza, M. S. Bonilla, L. T. Buchman, A. Ceja, H. Chaudhary, Y. Chen, M. Corman, K. Z. Csukás, C. M. Ferrus, S. E. Field, M. Giesler, S. Habib, F. Hébert, D. A. Hemberger, D. A. B. Iozzo, T. Islam, K. Z. Jones, A. Khairnar, L. E. Kidder, T. Knapp, P. Kumar, G. Lara, O. Long, G. Lovelace, S. Ma, D. Melchor, M. Morales, J. Moxon, P. J. Nee, K. C. Nell, E. O'Shea, S. Ossokine, R. Owen, H. P. Pfeiffer, I. G. Pretto, T. Ramirez-Aguilar, A. Ramos-Buades, A. Ravichandran, A. Ravishankar, S. Rodriguez, H. R. Rüter, J. Sanchez, M. A. Shaikh, D. Sun, B. Szilágyi, D. Tellez, S. A. Teukolsky, S. Thomas, W. Throwe, V. Varma, N. L. Vu, M. Walker, N. A. Wittek, and J. Yoo, "The sxs collaboration's third catalog of binary black hole simulations," 2025.
[71] M. Fernando, D. Neilsen, H. Lim, E. Hirschmann, and H. Sundar, "Massively Parallel Simulations of Binary Black Hole Intermediate-Mass-Ratio Inspirals," *SIAM J. Sci. Comput.* **41** (2019), no. 2, C97–C138, 1807.06128.
[72] C. O. Lousto and J. Healy, "Exploring the Small Mass Ratio Binary Black Hole Merger via Zeno's Dichotomy Approach," *Phys. Rev. Lett.* **125** (2020), no. 19, 191102, 2006.04818.
[73] N. A. Wittek, L. Barack, H. P. Pfeiffer, A. Pound, N. Deppe, L. E. Kidder, A. Macedo, K. C. Nelli, W. Throwe, and N. L. Vu, "Relieving Scale Disparity in Binary Black Hole Simulations," *Phys. Rev. Lett.* **134** (2025), no. 25, 251402, 2410.22290.
[74] M. Dhesi, H. R. Rüter, A. Pound, L. Barack, and H. P. Pfeiffer, "Worldtube excision method for intermediate-mass-ratio inspirals: Scalar-field toy model," *Phys. Rev. D* **104** (2021), no. 12, 124002, 2109.03531.
[75] S. A. Hughes, N. Warburton, G. Khanna, A. J. K. Chua, and M. L. Katz, "Adiabatic waveforms for extreme mass-ratio inspirals via multivoice decomposition in time and frequency," *Phys. Rev. D* **103** (2021), no. 10, 104014, 2102.02713. [Erratum: Phys.Rev.D 107, 089901 (2023)].

[76] Y.-X. Wei, X.-L. Zhu, J.-d. Zhang, and J. Mei, "Toward second-order self-force for eccentric extreme-mass ratio inspirals in Schwarzschild spacetimes," *Phys. Rev. D* **112** (2025), no. 6, 064048, 2504.09640.

[77] A. J. K. Chua, M. L. Katz, N. Warburton, and S. A. Hughes, "Rapid generation of fully relativistic extreme-mass-ratio-inspiral waveform templates for LISA data analysis," *Phys. Rev. Lett.* **126** (2021), no. 5, 051102, 2008.06071.

[78] L. Speri, M. L. Katz, A. J. K. Chua, S. A. Hughes, N. Warburton, J. E. Thompson, C. E. A. Chapman-Bird, and J. R. Gair, "Fast and Fourier: Extreme Mass Ratio Inspiral Waveforms in the Frequency Domain," (7, 2023) 2307.12585.

[79] J. Mathews, B. Wardell, A. Pound, and N. Warburton, "Post-adiabatic self-force waveforms: slowly spinning primary and precessing secondary," (10, 2025) 2510.16113.

[80] K. G. e. a. Arun, "New horizons for fundamental physics with lisa," *Living Reviews in Relativity* **25** (June, 2022).

[81] P. e. a. Amaro-Seoane, "Astrophysics with the laser interferometer space antenna," *Living Reviews in Relativity* **26** (Mar., 2023).

[82] S. Isoyama, R. Fujita, A. J. K. Chua, H. Nakano, A. Pound, and N. Sago, "Adiabatic waveforms from extreme-mass-ratio inspirals: an analytical approach," (11, 2021) 2111.05288.

[83] O. Burke, G. A. Piovano, N. Warburton, P. Lynch, L. Speri, C. Kavanagh, B. Wardell, A. Pound, L. Durkan, and J. Miller, "Assessing the importance of first postadiabatic terms for small-mass-ratio binaries," *Phys. Rev. D* **109** (2024), no. 12, 124048, 2310.08927.

[84] H. Khalvati, P. Lynch, O. Burke, L. Speri, M. van de Meent, and Z. Nasipak, "Systematic errors in fast relativistic waveforms for Extreme Mass Ratio Inspirals," (9, 2025) 2509.08875.

[85] R. Fujita, W. Hikida, and H. Tagoshi, "An Efficient Numerical Method for Computing Gravitational Waves Induced by a Particle Moving on Eccentric Inclined Orbits around a Kerr Black Hole," *Prog. Theor. Phys.* **121** (2009) 843–874, 0904.3810.

[86] Z. Nasipak, "pybhpt."

[87] B. Wardell, N. Warburton, K. Cunningham, L. Durkan, B. Leather, Z. Nasipak, C. Kavanagh, A. Ottewill, M. Casals, T. Torres, J. Neef, and S. Barsanti, "Teukolsky," feb, 2025. 10.5281/zenodo.14788956.

[88] M. van de Meent, "Gravitational self-force on generic bound geodesics in Kerr spacetime," *Phys. Rev. D* **97** (2018), no. 10, 104033, 1711.09607.

[89] Z. Nasipak, "Metric reconstruction and the Hamiltonian for eccentric, precessing binaries in the small-mass-ratio limit," (7, 2025) 2507.07746.

[90] L. V. Drummond, P. Lynch, A. G. Hanselman, D. R. Becker, and S. A. Hughes, "Extreme mass-ratio inspiral and waveforms for a spinning body into a Kerr black hole via osculating geodesics and near-identity transformations," *Phys. Rev. D* **109** (2024), no. 6, 064030, 2310.08438.

[91] A. M. Grant, "Flux-balance laws for spinning bodies under the gravitational self-force," *Phys. Rev. D* **111** (2025), no. 8, 084015, 2406.10343.

[92] V. Witzany, V. Skoupý, L. C. Stein, and S. Tanay, "Actions of spinning compact binaries: Spinning particle in Kerr matched to dynamics at 1.5 post-Newtonian order," *Phys. Rev. D* **111** (2025), no. 4, 044032, 2411.09742.

[93] G. A. Piovano, C. Pantelidou, J. Mac Uilliam, and V. Witzany, "Spinning particles near Kerr black holes: Orbits and gravitational-wave fluxes through the Hamilton-Jacobi formalism," *Phys. Rev. D* **111** (2025), no. 4, 044009, 2410.05769.

[94] V. Skoupý and V. Witzany, "Analytic Solution for the Motion of Spinning Particles in Kerr Spacetime," *Phys. Rev. Lett.* **134** (2025), no. 17, 171401, 2411.16855.

[95] M. Boyle *et al.*, "The SXS Collaboration catalog of binary black hole simulations," *Class. Quant. Grav.* **36** (2019), no. 19, 195006, 1904.04831.

[96] A. Buonanno and T. Damour, "Effective one-body approach to general relativistic two-body dynamics," *Phys. Rev. D* **59** (1999) 084006, gr-qc/9811091.

[97] T. Damour, "Gravitational Self Force in a Schwarzschild Background and the Effective One Body Formalism," *Phys. Rev. D* **81** (2010) 024017, 0910.5533.

[98] L. Barack, T. Damour, and N. Sago, “Precession effect of the gravitational self-force in a Schwarzschild spacetime and the effective one-body formalism,” *Phys. Rev. D* **82** (2010) 084036, 1008.0935.

[99] S. Akcay, L. Barack, T. Damour, and N. Sago, “Gravitational self-force and the effective-one-body formalism between the innermost stable circular orbit and the light ring,” *Phys. Rev.* **D86** (2012) 104041, 1209.0964.

[100] D. Bini and T. Damour, “High-order post-Newtonian contributions to the two-body gravitational interaction potential from analytical gravitational self-force calculations,” *Phys. Rev. D* **89** (2014), no. 6, 064063, 1312.2503.

[101] D. Bini and T. Damour, “Gravitational self-force corrections to two-body tidal interactions and the effective one-body formalism,” *Phys. Rev. D* **90** (2014), no. 12, 124037, 1409.6933.

[102] S. Bernuzzi, A. Nagar, T. Dietrich, and T. Damour, “Modeling the Dynamics of Tidally Interacting Binary Neutron Stars up to the Merger,” *Phys. Rev. Lett.* **114** (2015), no. 16, 161103, 1412.4553.

[103] S. Akcay and M. van de Meent, “Numerical computation of the effective-one-body potential q using self-force results,” *Phys. Rev. D* **93** (2016), no. 6, 064063, 1512.03392.

[104] D. Bini, T. Damour, and A. Geralico, “Spin-dependent two-body interactions from gravitational self-force computations,” *Phys. Rev. D* **92** (2015), no. 12, 124058, 1510.06230. [Erratum: Phys.Rev.D 93, 109902 (2016)].

[105] D. Bini, T. Damour, and A. Geralico, “Confirming and improving post-Newtonian and effective-one-body results from self-force computations along eccentric orbits around a Schwarzschild black hole,” *Phys. Rev. D* **93** (2016), no. 6, 064023, 1511.04533.

[106] C. Kavanagh, D. Bini, T. Damour, S. Hopper, A. C. Ottewill, and B. Wardell, “Spin-orbit precession along eccentric orbits for extreme mass ratio black hole binaries and its effective-one-body transcription,” *Phys. Rev. D* **96** (2017), no. 6, 064012, 1706.00459.

[107] A. Nagar *et al.*, “Time-domain effective-one-body gravitational waveforms for coalescing compact binaries with nonprecessing spins, tides and self-spin effects,” *Phys. Rev. D* **98** (2018), no. 10, 104052, 1806.01772.

[108] A. Nagar, F. Messina, C. Kavanagh, G. Lukes-Gerakopoulos, N. Warburton, S. Bernuzzi, and E. Harms, “Factorization and resummation: A new paradigm to improve gravitational wave amplitudes. III: the spinning test-body terms,” *Phys. Rev. D* **100** (2019), no. 10, 104056, 1907.12233.

[109] A. Antonelli, M. van de Meent, A. Buonanno, J. Steinhoff, and J. Vines, “Quasicircular inspirals and plunges from nonspinning effective-one-body Hamiltonians with gravitational self-force information,” *Phys. Rev. D* **101** (2020), no. 2, 024024, 1907.11597.

[110] M. van de Meent, A. Buonanno, D. P. Mihaylov, S. Ossokine, L. Pompili, N. Warburton, A. Pound, B. Wardell, L. Durkan, and J. Miller, “Enhancing the SEOBNRv5 effective-one-body waveform model with second-order gravitational self-force fluxes,” *Phys. Rev. D* **108** (2023), no. 12, 124038, 2303.18026.

[111] B. Leather, A. Buonanno, and M. van de Meent, “Inspiral-merger-ringdown waveforms with gravitational self-force results within the effective-one-body formalism,” *Phys. Rev. D* **112** (2025), no. 4, 044012, 2505.11242.

[112] E. A. Huerta, C. Moore, P. Kumar, D. George, A. J. Chua, R. Haas, E. Wessel, D. Johnson, D. Glennon, A. Rebei, A. M. Holgado, J. R. Gair, and H. P. Pfeiffer, “Eccentric, nonspinning, inspiral, Gaussian-process merger approximant for the detection and characterization of eccentric binary black hole mergers,” *Phys. Rev. D* **97** (2018), no. 2, 024031, 1711.06276.

[113] K. Paul, A. Maurya, Q. Henry, K. Sharma, P. Satheesh, Divyajyoti, P. Kumar, and C. K. Mishra, “Eccentric, spinning, inspiral-merger-ringdown waveform model with higher modes for the detection and characterization of binary black holes,” *Phys. Rev. D* **111** (2025), no. 8, 084074, 2409.13866.

[114] T. Damour and A. Nagar, “Faithful effective-one-body waveforms of small-mass-ratio coalescing black-hole binaries,” *Phys. Rev. D* **76** (2007) 064028, 0705.2519.

[115] N. Yunes, A. Buonanno, S. A. Hughes, Y. Pan, E. Barausse, M. C. Miller, and W. Throwe, “Extreme Mass-Ratio Inspirals in the Effective-One-Body Approach: Quasi-Circular, Equatorial Orbits around

a Spinning Black Hole," *Phys. Rev. D* **83** (2011) 044044, 1009.6013. [Erratum: Phys.Rev.D 88, 109904 (2013)].

[116] A. Taracchini, A. Buonanno, G. Khanna, and S. A. Hughes, "Small mass plunging into a Kerr black hole: Anatomy of the inspiral-merger-ringdown waveforms," *Phys. Rev. D* **90** (2014), no. 8, 084025, 1404.1819.

[117] A. Nagar and S. Albanesi, "Toward a gravitational self-force-informed effective-one-body waveform model for nonprecessing, eccentric, large-mass-ratio inspirals," *Phys. Rev. D* **106** (2022), no. 6, 064049, 2207.14002.

[118] S. Albanesi, S. Bernuzzi, T. Damour, A. Nagar, and A. Placidi, "Faithful effective-one-body waveform of small-mass-ratio coalescing black hole binaries: The eccentric, nonspinning case," *Phys. Rev. D* **108** (2023), no. 8, 084037, 2305.19336.

Université Libre de Bruxelles, Av. Franklin Roosevelt, 50, 1050 Brussels, Belgium
Email address: geoffrey.compere@ulb.be

BUILDING AN EFFICIENT EMRI SEARCH ALGORITHM

CURT CUTLER

Keywords: Laser Interferometer Space Antenna, Extreme-Mass-Ratio Inspiral

1. INTRODUCTION

This is a summary of the talk of the same title) that I gave in Singapore in Aug., 2025. The talk consisted of two main parts. The first was an overview of the EMRI extreme-mass ratio inspiral) search problem where here ”search” includes both detection and parameter estimation), starting with why it is a hard problem, then summarizing the current state of the art, and ending with a menu of ideas and techniques that prospective LISA data analysts will be drawing from in constructing EMRI search algorithms. The second main part was a presentation of my own recent work in this subject: I have constructed a set of phenomenological templates based on Chebyshev polynomials, to be used in the ”detection” stage of the search.

2. OVERVIEW OF THE EMRI SEARCH PROBLEM

2.1. **Why the EMRI search problem is hard** The problem is hard for several reasons. First, the correct EMRI waveforms to be used as templates in some version of matched-filter search) are long-lived typically a year or more in-band), quite complicated, and expensive to calculate. Progress towards calculating the templates efficiently was one of the main topics of the whole meeting.) Second, a truly vast number of them– crudely estimated to be of order 10^4 – would need to be searched over in a straightforward grid search. Of course, that just means that a straightforward grid search is completely impractical – hence the need for cleverer approach. The third big problem is the huge number of near-degeneracies; as shown in [1], the likelihood function is extremely multimodal, with parameter-space points of high likelihood existing far away 100 and more) from the true parameters of the signal.

2.2. **Current state of the art** I explained that prior to 2011, there had been steady progress in constructing an efficient EMRI search algorithm, but that work in this area had then almost ceased for a decade, picking back up around 2022. I gave my opinion that algorithm developed by Strub et al. 2025)represented the current state of the art [2], but was still along way from what the community needs to develop. Since this Singapore meeting there has appeared a new paper, [3], which represents a significant step forward, and which is now in my opinion) the state of the art.

Overall Method	Search Statistic (main goal is usually to broaden the peaks)	other Tools&Tricks, espec for speed-up; use as many as you can!
--Stochastic Methods, espec. various flavors of MCMC, e.g., parallel-tempering --Grid-based, hierarchical searches, e.g., most sensitive CW search --Machine Learning, e.g., convolutional neural network, used in Cole et al. (2025) --Other global optimization methods, e.g., differential evolution, used in Strub et al. (2025)	--the usual likelihood, but starting with some piece of the signal, and/or reduced parameter space --semi-coherent "SNR" , e.g., most sensitive CW search --power along track in f-t plane; Strub et al. (2025) use clever variation on this --statistic that down-weights all the (merely) local maxima, e.g., one-stop function of Chua (2022)	--FFT trick for searching over time-slides of template, e.g. template-based compact-binary searches --heterodyning (both the data and the likelihood evaluation) --F-statistic, and variations, for analytically maximizing over some extrinsic params --start by processing data into short FFT database, or similar --fast waveform production, espec. FEW code --phenomenological templates, e.g. Taylor-based or Chebyshev-based expansions

FIGURE 1. EMRI Search Menu. The first column is a list of overarching search methods, the second column is a list of search statistics for use in early stages of the search, and the final column is a collection of useful ”tricks”, mostly for improving computational efficiency.

2.3. **Menu of Tools and Techniques** EMRI searchers can draw on a great deal of related work on other computationally-limited searches, especially the search for so-called ”continuous GW” searches in ground-based data. I assembled a ”menu” of ideas/methods that EMRI searchers can draw from, which is shown in Fig. 1.

3. PHENOMENOLOGICAL TEMPLATES BASED ON THE CHEBYSHEV EXPANSION

3.1. **Motivations** There were two main motivations for my work on the Chebyshev expansion of single-harmonic EMRI waveforms. First, I wanted to build a search algorithm on the following idea: start the search by looking only for the dominant harmonic often the [2,0,0] harmonic), and only in a few mHz band around the ”sweet spot” of the LISA noise curve–say, the band $3 \quad 8$ mHz. Second, I found that the phase as a function of time or frequency of) this and other harmonics could be captured to high precision, over the given frequency range, by just 5 terms in a Chebyshev expansion. Therefore I could use just the first 5 Chebyshev polynomials to construct accurate single-harmonic waveform templates, with the coefficients of the Chebyshev coefficients being the new phenomenological parameters. And these phenomenological templates are very inexpensive to construct, computationally.

3.2. **A few more details on the method** Let $t(f)$ be the time-frequency track of one of the dominant harmonics. Basically, we have shown that it is generally possible to fit $\ln(dt/df)$ to high accuracy using just the first 5 terms in a Chebyshev expansion. From that, we can obtain the phase (f) of the Fourier transform $\tilde{h}(f)$ by integrating dt/df twice.

3.3. **A brief summary of results** I presented a couple kinds of results. First, I showed that for each of the top 3 most important harmonics, the *match* between the true waveform for that one harmonic) and its 5-term Chebyshev is typically 0.99. I was also able to use this parametrization to "count" the number of templates required to cover the parameter space, when the signal was restricted to a single harmonic and restricted to the band $3 \quad 8$ mHz. The answers depends a bit on which harmonic is considered, but are in the range $\sim 10^{13} \quad 10^{14}$ not including time-slides), so these restrictions reduce the size of the space by more than a factor 10^2, compared to the estimate in the Introduction.

Acknowledgments

This research was carried out at the Jet Propulsion Laboratory JPL), California Institute of Technology, under a contract with the National Aeronautics and Space Administration 80NM0018D0004).

REFERENCES

[1] Alvin J.K. Chua and Curt J. Cutler. "Nonlocal parameter degeneracy in the intrinsic space of gravitational-wave signals from extreme-mass-ratio inspirals." Physical Review D 106, no. 12 2022): 124046. Nonlocal parameter degeneracy in the intrinsic space of gravitational-wave signals from extreme-mass-ratio inspirals *Physical Review* , 106, 124046, 2022.

[2] Stefan H. Strub, Lorenzo Speri, and Domenico Giardini Searching for extreme mass ratio inspirals in LISA: from identification to parameter estimation *arXiv*, 2505.17814, 2025.

[3] Lorenzo Speri, Rodrigo Tenorio, Christian Chapman-Bird, and Davide Gerosa. Ab uno disce omnes: Single-harmonic search for extreme mass-ratio inspirals em arXiv preprint arXiv:2510.20891 2025).

JET PROPULSION LABORATORY, CALIFORNIA INSTITUTE OF TECHNOLOGY
Email address: cutler@tapir caltech edu

METRIC RECONSTRUCTION ON KERR SPACETIME IN LORENZ GAUGE

SAM R. DOLAN

Classification AMS 2020: 83C57; 83C35; 70F05.

Keywords: General relativity; Black holes; Gravitational waves; Two-body problems.

The context of the workshop, and of my talk, is the two-body problem in general relativity, in which a compact body of mass m_2 orbits around a spinning black hole of mass m_1. This system loses energy through emission of gravitational radiation, leading to the eventual coalescence of the pair. In principle, the emitted gravitational wave signal encodes information about the orbit and the spacetime that can be used to test general relativity and its extensions, as well as to probe the environments of supermassive black holes. Ground-based gravitational-wave detectors have detected more than 200 "chirps" from *comparable-mass* binaries ($m_2/m_1 \lesssim 1/100$) since 2015 (see recent GWTC-4 results from the LIGO/Virgo collaboration). A space-based detector, the Laser Interferometer Space Antenna (LISA), due to launch in the 2030s, will detect signals from Extreme Mass-Ratio Inspirals (EMRIs) with much smaller mass-ratios $m_2/m_1 \ll 1/1000$.

In the Gravitational Self-Force framework, one takes a perturbative approach [1]. The spacetime metric of the primary serves as the 'background' on which one calculates a force F_μ that pushes the secondary's *worldline* away from a background geodesic. The force F_μ (defined via a regularization procedure) is calculated from first-derivatives of the *metric perturbation* generated by the secondary. The metric perturbation $h_{\mu\nu}$ on a Kerr black hole background is governed by 10 coupled PDEs that appear rather fiendish; and there is also substantial freedom in the choice of *gauge* (i.e. in coordinate choice at perturbative order) that affects F_μ itself.

In the 1970s, Teukolsky [2] showed that a certain pair of Weyl scalars, derived from projections of the Weyl tensor onto the principal null tetrad, satisfy *decoupled* PDEs, and moreover these PDEs are *separable* into ODEs. A natural question arose: how can one reconstruct the metric perturbation in a convenient gauge from these scalar quantities?

The standard CCK (Chrzanowski-Cohen-Kegeles) metric reconstruction procedure [3] generates a *vacuum* ($T_{\mu\nu} = 0$) metric perturbation $h_{\mu\nu}$ from a Weyl scalar Ψ_0 (via a Hertz potential) in *radiation gauge*: $h_{\mu\nu}l^\nu = 0$. However, in the presence of sources ($T_{\mu\nu} \neq 0$) on worldlines, "glueing" such vacuum solutions together leads to gauge singularities that are extended (i.e. not confined to the worldline). This presents a practical problem for second-order calculations, since quadratic combinations of the first-order metric perturbation (and its derivatives) generate the second-order source, worsening any spurious singular features.

To address this problem, Green, Hollands and Zimmerman [4] introduced a "corrector tensor" determined from transport equations on null rays. My collaborators and I took an alternative approach, by seeking to cast the metric perturbation into *Lorenz gauge* ($\nabla_\mu \bar{h}^{\mu\nu} = 0$) which has the following desirable properties: (1) the linearized Einstein

Date: 16th January 2026.

equation is hyperbolic (i.e. solutions are wave-like); (2) the metric perturbation diverges in an isotropic fashion, as $1/(\text{proper distance})$, near the secondary's worldline; (3) the second-order calculation for Schwarzschild (non-spinning) uses this gauge, and there there is comparison data available on Kerr from a time-domain code.

In my talk I described progress towards calculating high-quality Lorenz-gauge metric perturbation data: a key input for perturbative calculations that will underpin accurate waveform modelling for LISA, at second order in the Gravitational Self-Force expansion (i.e. in powers of m_2/m_1) and at first Post-Adiabatic order. The approach is based on metric reconstruction in Lorenz gauge from *six* Teukolsky-like scalar variables in the frequency domain. These six scalars satisfy separable, decoupled equations of second order. Of the six, two are Weyl scalars (of spin-weight ± 2), two are Maxwell-like scalars (of spin-weights ± 1), and the remaining two – the trace h and an auxiliary scalar κ – are of spin-weight zero. In vacuum regions, the Teukolsky-Starobinskii identities – which relate Teukolsky variables of opposite spin-weight – reduce the system to four equations.

We now have a general formulation for computing the non-static Lorenz-gauge metric perturbation generated by a secondary on generic (non-circular, non-equatorial) bound orbits, and full implementation is underway. In the first paper [5], we showed how to apply (high-order) differential operators to convert from radiation gauge to Lorenz gauge *in vacuum regions* in the spin-2 sector; and we derived a complete set of Lorenz-gauge modes in the spin-1 and spin-0 sectors; and completion pieces (i.e. mass and angular momentum perturbations). In the second paper [6], we 'matched' inner and outer solutions on the sphere at $r = r_0$ to obtain the metric perturbation for a secondary on a circular equatorial orbit at radius r_0. In the third paper [7], we showed that the general solution of Aksteiner, Andersson, and Bächdahl [8] – which satisfies the *sourced* linearised Einstein equation – can be rendered in Lorenz gauge, and in doing so we derived the source terms for all six scalar equations in terms of differential operators acting on the stress-energy tensor $T_{\mu\nu}$.

The data for the circular-orbit metric perturbation forms part of the input for a second-order self-force calculation now in progress. Moreover, this data has also been used as input for assessing the effect of a black hole environment on EMRIs, particularly in the (fascinating-but-speculative) scenario in which the black hole is embedded in a scalar field 'cloud' generated by black hole superradiance [9].

There are still remaining challenges, however. Whereas five of the six scalars have compact sources, confined to the secondary's worldline, the sixth, κ, has an extended source proportional to the trace, of the form

$$\Box\kappa = \frac{1}{2}h + (\text{compact source}). \tag{0.1}$$

This makes it more challenging to compute. Separately, the transformation to Lorenz gauge breaks down in the static limit ($\omega = 0$), and so the static sector requires additional consideration. In the absence of a full solution here, a valid approach is to seek to match up vacuum solutions on either side of the worldline, as in our second paper [6]. But to extend the matching approach to eccentric or generic orbits, a more systematic approach is needed, and addressing this problem was the main new content in my talk.

I described a new approach called the *Homogeneous Mode Matching (HMM) method*[1] that builds upon the method of Extended Homogeneous Solutions (EHS) [10].

To illustrate the HMM method, suppose we have a scalar field Φ on Schwarzschild spacetime, generated by a scalar charge q on a worldline $\gamma : x_0(\tau)$. After decomposing Φ in spherical harmonics, we have a 1+1D PDE schematically of the form $\hat{\mathcal{D}}\psi = \mathcal{S}\delta(r - r_0(\tau))$, and we can write its solution as

$$\psi(t, r) = \psi^+(t, r)\Theta[r - r_0(\tau)] + \psi^-(t, r)\Theta[r_0(\tau) - r], \tag{0.2}$$

where $\psi^\pm$ are inner and outer *homogeneous solutions*, and $\Theta[\cdot]$ is the Heaviside step function. From the PDE, it is straightforward to deduce the *jump conditions* satisfied by $\psi^\pm$ at the worldline, namely

$$[\psi] = 0, \quad [\partial_r\psi] = J_r(\tau), \tag{0.3}$$

where $J_r(\tau)$ is a function on the worldline, and $[\psi] = \lim_{\epsilon\to0^+}(\psi(t, r_0 + \epsilon) - \psi(t, r_0 - \epsilon))$.

The next step in the HMM method is to decompose the homogeneous solutions $\psi^\pm$ as Fourier series in the frequency domain. For an eccentric equatorial orbit,

$$\psi^\pm(t, r) = \sum_{n=-\infty}^{\infty} c_n^\pm \hat{\psi}_n^\pm(r) e^{-i\omega_{mn}t}, \quad \omega_{mn} = m\Omega_\phi + n\Omega_r, \tag{0.4}$$

where $\Omega_{\phi/r}$ are the azimuthal/radial frequencies, and $\hat{\psi}(r)$ satisfy homogeneous ODEs with standard IN/UP boundary conditions. In practice, the n-sum is taken over a finite range $[n_{\text{min}}, n_{\text{max}}]$, due to exponential convergence of Fourier sums for smooth functions.

By evaluating the jump conditions at a sample of times $\{t_k\}$ on the worldline we obtain a linear system $Ax = b$ for the unknowns $\{c_n^\pm\}$. The matrix A need not be square; I find it advantageous to over-sample so that the number of equations exceeds the number of unknowns. I used the Black Hole Perturbation Toolkit to calculate the homogeneous mode functions $\hat{\psi}(r)$, and `LeastSquares` in Mathematica to solve the linear system for $c_n^\pm$. The numerical results for $c_n^\pm$ obtained via the HMM method compared very well with those obtained by evaluating the integrals in the EHS method (an extension of the standard Variation of Parameters method, employing analytic continuation to evade the Gibbs phenomenon) [10]. An absolute difference of less than 10^{-12} was obtained. The HMM method also seems to be more efficient, since it does not require the evaluation of integrals, although this remains to be properly quantified.

Importantly, the HMM method can be applied to cases where the system does not fully decouple, or where the source term is not known. It can also be used for coupled PDEs where the principal part of the PDE decouples, but the lower-order parts do not. This makes it suitable for matching vacuum solutions in the static sector. Work in implementing the HMM method for various scenarios is being taken forward by K. Cunningham. At the time of writing, Mr Cunningham has obtained promising preliminary results for scalar fields on Kerr, and for $s = \pm2$ Teukolsky scalars, by using this method. However, extending to unbound scattering trajectories is anticipated to be more challenging.

[1] In this talk I amused myself by referring to it as the *"Nature Adores a Vacuum"* method

References

[1] L. Barack and A. Pound, "Self-force and radiation reaction in general relativity," Rept. Prog. Phys. **82** (2019) 016904 [arXiv:1805.10385].

[2] S. A. Teukolsky, "Rotating black holes - separable wave equations for gravitational and electromagnetic perturbations," Phys. Rev. Lett. **29** (1972), 1114-1118.

[3] P. L. Chrzanowski, "Vector potential and metric perturbations of a rotating black hole," Phys. Rev. D **11** (1975), 2042-2062.

[4] S. R. Green, S. Hollands and P. Zimmerman, "Teukolsky formalism for nonlinear Kerr perturbations," Class. Quant. Grav. **37** (2020) 075001 [arXiv:1908.09095].

[5] S. R. Dolan, C. Kavanagh and B. Wardell, "Gravitational perturbations of rotating black holes in Lorenz gauge," Phys. Rev. Lett. **128** (2022) 151101 [arXiv:2108.06344].

[6] S. R. Dolan, L. Durkan, C. Kavanagh and B. Wardell, "Metric perturbations of Kerr spacetime in Lorenz gauge: circular equatorial orbits," Class. Quant. Grav. **41** (2024) 155011 [arXiv:2306.16459].

[7] B. Wardell, C. Kavanagh and S. R. Dolan, "Sourced metric perturbations of Kerr spacetime in Lorenz gauge," Class. Quant. Grav. **42** (2025) 205007 [arXiv:2406.12510].

[8] S. Aksteiner, L. Andersson and T. Bäckdahl, "New identities for linearized gravity on the Kerr spacetime," Phys. Rev. D **99** (2019) 044043 [arXiv:1601.06084].

[9] C. Dyson, T. F. M. Spieksma, R. Brito, M. van de Meent and S. Dolan, "Environmental Effects in Extreme-Mass-Ratio Inspirals: Perturbations to the Environment in Kerr Spacetimes," Phys. Rev. Lett. **134** (2025) 211403 [arXiv:2501.09806].

[10] L. Barack, A. Ori and N. Sago, "Frequency-domain calculation of the self force: The High-frequency problem and its resolution," Phys. Rev. D **78** (2008), 084021 [arXiv:0808.2315].

School of Mathematical and Physical Sciences, University of Sheffield, Sheffield, U.K.
Email address: `s.dolan@sheffield.ac.uk`

WHY MATTER MATTERS: ASTROPHYSICAL ENVIRONMENTS OF EMRIS

LISA DRUMMOND

EMRIs are powerful probes of strong-field gravity and galactic nuclei. While often modeled in vacuum, real EMRIs form and evolve in complex astrophysical environments. This talk reviews the role of matter (including accretion disks, dark matter, and stellar backgrounds) in shaping EMRI dynamics and gravitational wave signals. I highlight recent progress and open questions, and discuss the implications for detection with LISA. I also explore the emerging connection between EMRIs and quasi-periodic eruptions (QPEs), whose timing may encode signatures of inspiraling compact objects interacting with accretion disks.

California Institute of Technology, USA
Email address: `lisadrum@caltech.edu`

THE PROSPECTS AND CHALLENGES OF SCIENCE WITH LISA EMRI OBSERVATIONS

JONATHAN GAIR

Classification AMS 2020: 62F15, 83B05, 85A05

Keywords: gravitational waves, black holes, data analysis, extreme-mass-ratio inspirals

Extreme-mass-ratio inspirals (EMRIs), the inspirals and mergers of compact objects (usually black holes but white dwarfs or neutron stars are also possible) with a massive black hole (MBH) in the centre of a galaxy, are a key source for the future space-based gravitational wave (GW) detector LISA [1], recently officially adopted by ESA and due to be launched in 2035. A typical EMRI generates many hundreds of thousands of cycles of gravitational radiation detectable by LISA, all of which are generated while the small object is very close to the central black hole. This signal thus encodes detailed information about the properties of the black hole and its immediate environment [2].

EMRIs may form in a number of different ways. The classic channel is driven by two-body relaxation. MBHs in galactic centres are usually surrounded by a cluster of stars. These stars interact with each other gravitationally, and close encounters can perturb the orbits of compact objects so that they pass very close to the central MBH. If this happens, energy and angular momentum are radiated from the orbit into GWs, leaving the compact object on an orbit that is bound to the MBH. The compact object then gradually inspirals into the central MBH via GW emission, eventually forming an EMRI. This details of this process depend on the physics of nuclear stellar clusters (see [3] for more details). Other EMRI formation channels include the Hills mechanism [4], in which a binary star system is tidally disrupted when it passes close enough to the MBH, ejecting one component as a hypervelocity star and leaving the other bound to the central black hole where it becomes an EMRI, or the tidal stripping of a giant star. In the latter case, the envelope of the giant star is removed by the tidal interaction, and the core of the star is then left on an orbit around the black hole such that it eventually inspirals as an EMRI [5]. Stars might also form directly in-situ in the vicinity of a black hole via fragmentation of a massive accretion disc [6], with their remnants becoming EMRIs.

This variety in formation channels offers uncertainty for LISA, but also highlights the discovery potential of the mission, as LISA will provide the first measurements of the relative rates of EMRIs from these different channels. Over recent years, we have also made electromagnetic observations of systems that are believed to be related to EMRIs. Around 20 hypervelocity stars have been observed in our galaxy whose trajectories are consistent with formation via the Hills mechanism in the Galactic centre or in the centre of the Large Magellanic Cloud [7]. In addition, transient electromagnetic emission from MBHs has been observed that is believed to be associated with the same dynamical processes that create EMRIs. This includes tidal disruption events, which are the detonations of stars perturbed onto orbits that pass close to MBHs, and quasi-periodic eruptions/oscillations (QPEs/QPOs). The leading model to explain QPEs is that the emission is triggered by a compact object orbiting close to the MBH passing through the accretion disc of the MBH as it orbits [8]. Objects on such orbits will later become EMRIs, offering the prospect of multimessenger observations of the same system [9]. These electromagnetic observations have provided EMRI rate estimates that are consistent with theoretical models, providing greater confidence that LISA will observe a significant number of EMRI events over the mission lifetime.

Estimating how many EMRI events that LISA will observe requires three ingredients — the rate of EMRIs in galactic nucleii, as a function of the MBH properties; the number density of black holes in the range $10^4 M_\odot \lesssim M \lesssim 10^7 M_\odot$ to which LISA is sensitive; and the detectability of EMRIs in LISA data, as a function of the system parameters. There are large uncertainties in the first two ingredients in particular. For the rate per galaxy, uncertainties arise not only because of the variety of different EMRI formation channels, but also because the physics of stellar clusters is complex and difficult to simulate. Matching of scales between the Newtonian many body dynamics that dominates far from the black hole, and the relativistic dynamics in the close vicinity of the MBH, create computational difficulties that lead to large uncertainties in predicting the proportion of compact objects passing close to the MBH that plunge directly into the black hole rather than inspiraling. The rate at which compact objects are brought from larger radii in the galaxy to the vicinity of the MBH, to replenish the compact objects falling into the MBH, is also hard to model. The space density of MBHs in the mass range relevant to LISA is not much better constrained, as these MBHs are very difficult to observe electromagnetically, once again providing LISA with a rich discovery space at the cost of uncertain rate predictions. One thing comparatively well constrained is the sensitivity of LISA to EMRIs. Even there the signal-to-noise ratio required for a confident detection is not known, due to data analysis uncertainties, and computations rely on having models for the EMRI signals that are both physically accurate and sufficiently cheap to evaluate that the whole parameter space can be explored. EMRI waveform modelling is a subject of intense study, as reported elsewhere at this meeting, and fast, physically accurate models are now available [10], but only for a restricted portion of the parameter space. Approximate models [11] must therefore be used to assess the EMRI detection horizon, introducing a factor of two uncertainty in the rates. Given all these uncertainties the estimated EMRI detection rate ranges from a few to a few thousand events per year [12], with a best guess of ~ 100 EMRIs yr^{-1}. Recent work has attempted to address some of the astrophysical uncertainties [13]. This has not significantly changed the rate estimates, but has found that the ratio of inspirals to direct plunges might be higher than previously thought, and EMRIs may have higher residual eccentricity at plunge [14], creating further modelling challenges.

Hundreds of EMRI observations would offer a rich range of possibilities for science. The $\sim 10^5$ waveform cycles observable from a typical EMRI allow the parameters of the system to be measured with unprecedented accuracy. EMRI observations will constrain the intrinsic parameters of the system (mass and rotation rate of the MBH, mass of the smaller object, and properties of the orbit, such as inclination and eccentricity) to precisions of 10^{-6}–10^{-4}, sky locations to a few square degrees and luminosity distances to a few percent [12, 15]. These precisions arise from the large number of observed waveform cycles and are achieved even for events at the threshold of detection. Through these precise measurements, EMRI observations will provide unique information about the properties of quiescent MBHs in the relatively low redshift Universe, the relative importance of different EMRI formation channels and the physical processes that govern the dynamics in dense stellar systems [16]. In addition, EMRIs can probe the immediate astrophysical environments of their host MBH. As we know from observations of QPEs, EMRIs can occur around MBHs with accretion discs. When the smaller object passes through the MBH disc as it orbits, it experiences a drag which changes the orbital trajectory. In general, any effect that leads to a significant orbital dephasing over the observation can be detected, meaning effects at the level of 10^{-5}. It has been shown that EMRIs occurring in systems with discs can provide measurements of the disc density profile [17] and, for EMRIs on eccentric orbits that transition from supersonic to subsonic motion over the inspiral, also measurements of the disc viscosity and accretion rate [18]. For the same reason, EMRIs also provide very sensitive probes of the spacetime structure outside the MBH and can thus be used for fundamental physics, to test for consistency of the MBH geometry with that of a Kerr black hole, as predicted by GR. EMRIs are sensitive to the smallest absolute deviation of any GW probe. The natural ways to build alternative theories to GR are to include quadratic and higher order curvature terms in the action, or to introduce couplings to additional fields. EMRIs are not a particularly good probe of higher curvature deviations, as these are suppressed for MBHs relative to stellar-origin black holes. However, EMRIs are excellent probes of scalar-tensor theories of gravity, for which the signature is dominated by scalar charge accumulating on the small object, and therefore it is the curvature of the smaller black hole that is most important [19]. Finally, EMRIs can also be used as standard sirens, to probe the expansion history of the Universe, by combining the luminosity distance measurement from the GWs with an electromagnetic redshift. EMRIs are unlikely to have direct counterparts, so the most promising approach to cosmography is via cross-correlation of EMRI localisation volumes with galaxy catalogues. This could provide few percent measurements of the Hubble constant and ten percent measurements of Ω_m when all the EMRIs observed over the mission are combined. These constraints are further improved when combined with measurements from MBH binary mergers observed by LISA at higher redshift [20].

To realise this exciting scientific potential it is necessary to identify and characterise the EMRIs in the LISA data and this poses significant challenges. LISA will have a source-dominated data stream with thousands of sources of many different types simultaneously present and overlapping in time and frequency, the instrumental noise will not be known a priori and the data will be contaminated by glitches and gaps. These complexities mean that LISA data analysis requires a simultaneous *global fit* to all the sources of all the different types plus the instrumental noise. Global fits are under development by several groups and have successfully analysed simplified data containing only MBH binaries, galactic binaries and stationary Gaussian noise [21]. Inclusion of EMRIs in these fits poses additional challenges, since the same complexity of the EMRI signals that allows the remarkable precision of parameter measurement introduces a complex structure in the likelihood space, with many secondary modes and a primary mode occupying a tiny fraction of the prior volume [22]. The successful recovery of isolated EMRI signals in simplified data has already been demonstrated [23], and new searches are being developed designed to tackle more realistic data sets [24]. Over the coming decade we expect to bring these various pieces of work together into a final LISA global fit pipeline, able to find and fit all of the sources in the data. Then we will finally be ready to deliver the precision measurements required to realise LISA's revolutionary scientific potential.

References

[1] M. Colpi et al. LISA Definition Study Report *arXiv:*2402.07571

[2] J. Gair et al. Testing General Relativity with Low-Frequency, Space-Based Gravitational-Wave Detectors. *Liv. Rev. Rel.*, 16, 7 (2013).

[3] P. Amaro Seoane et al. Astrophysics with LISA *Liv. Rev. Rel.*, 26, 2 (2023).

[4] J. G. Hills Hyper-velocity and tidal stars from binaries disrupted by a massive Galactic black hole. *Nature*, 331, 687 (1988).

[5] P. Amaro Seoane et al. Intermediate and Extreme Mass-Ratio Inspirals – Astrophysics, Science Applications and Detection using LISA. *Class. Quant. Grav.*, 24, R113 (2007).

[6] Y. Levin. Formation of massive stars and black holes in self-gravitating AGN discs, and gravitational waves in LISA band. *arXiv*:astro-ph/0307084

[7] J. J. Han et al. Hypervelocity Stars Trace a Supermassive Black Hole in the Large Magellanic Cloud. *Astrophys. J.*, 982, 188 (2025).

[8] A. Franchini et al. Quasi-periodic eruptions from impacts between the secondary and a rigidly precessing accretion disc in an EMRI system. *Astron. & Astrophys.*, 675, A100 (2023).

[9] S. Kejriwal et al. Repeating nuclear transients as candidate electromagnetic counterparts of LISA extreme mass ratio inspirals. *Mon. Not. Roy. Astorn. Soc.*, 532, 2143 (2024).

[10] C. E. A. Chapman-Bird et al. The Fast and the Frame-Dragging: Efficient waveforms for asymmetric-mass eccentric equatorial inspirals into rapidly-spinning black holes. *arXiv*:2506.09470.

[11] A. Chua et al. The Fast and the Fiducial: Augmented kludge waveforms for detecting extreme-mass-ratio inspirals. *Phys. Rev.* D 96, 044005 (2017).

[12] S. Babak et al. Science with the space-based interferometer LISA. V: Extreme mass-ratio inspirals. *Phys. Rev.* D, 95, 103012 (2017).

[13] D. Mancieri et al. Hanging on the cliff: Extreme mass ratio inspiral formation with local two-body relaxation and post-Newtonian dynamics. *Astron. & Astrophys.*, 694, A272 (2025).

[14] D. Mancieri et al. Eccentricity distribution of extreme mass ratio inspirals. *arXiv*:2509.02394

[15] H. Khalvati et al. Impact of relativistic waveforms in LISA's science objectives with extreme-mass-ratio inspirals. *Phys. Rev.* D 111, 082010 (2025).

[16] J. Gair et al. LISA extreme-mass-ratio inspiral events as probes of the black hole mass function *Phys. Rev.* D 81, 104014 (2010).

[17] L. Speri et al. Probing Accretion Physics with Gravitational Waves. *Phys. Rev.* X 13, 021035 (2023).

[18] F. Duque et al. Constraining accretion physics with gravitational waves from eccentric extreme-mass-ratio inspirals. *Phys. Rev.* D 111, 084006 (2025).

[19] L. Speri et al. Probing fundamental physics with Extreme Mass Ratio Inspirals: a full Bayesian inference for scalar charge. *arXiv*:2406.07607.

[20] D. Laghi et al. Gravitational wave cosmology with extreme mass-ratio inspirals. *Mon. Not. Roy. Astron. Soc.* 508, 4512 (2021).

[21] M. Katz et al. An efficient GPU-accelerated multi-source global fit pipeline for LISA data analysis. *Phys. Rev.* D 111, 024060 (2025).

[22] A. J. K. Chua and C. J. Cutler Non-local parameter degeneracy in the intrinsic space of gravitational-wave signals from extreme-mass-ratio inspirals. *Phys. Rev.* D 106, 124046 (2022).

[23] S. Babak et al. An algorithm for detection of extreme mass ratio inspirals in LISA data. *Class. Quantum Grav.* 26, 135004 (2009).

[24] L. Speri et al. Ab uno disce omnes: Single-harmonic search for extreme mass-ratio inspirals. *arXiv*:2510.20891.

Max Planck Institute for Gravitational Physics (Albert Einstein Institute), Am Mühlenberg 1, 14476 Potsdam, Germany

Email address: jgair@aei.mpg.de

LISA AND THE LISA SCIENCE TEAM

ANNA HEFFERNAN
ON BEHALF OF THE LISA SCIENCE TEAM

Classification AMS 2020:

Keywords: LISA, Science Team, gravitational waves, waveforms, compact binaries

1. Abstract

LISA, the Laser Interferometer Space Antenna, due to launch mid-2035, is a large class space mission by the European Space Agency (ESA). In partnership with NASA and ESA-member states, ESA is on track to launch what is expected to be the first space-based gravitational wave detector. By hosting detectors in space, one gains access to a lower frequency band of gravitational wave sources and with them, a plethora of new science. To maximise this scientific gain, ESA and NASA selected 20 scientists for the LISA Science Team, to carry out and/or lead necessary actions on the run up to LISA launch. We give a short overview and update of the LISA mission, some of its science objectives and related waveforms, as well as the work of the LISA Science Team as of December 2025.

2. The LISA Mission

LISA will detect gravitational waves (GWs) in the mHz range, complementing current and future ground detectors; the mission and its objectives are fully described in the LISA Redbook [1]. LISA is a constellation of 3 spacecraft (SC) forming an almost equilateral triangle, inclined by 60 degrees to the orbital plane, whose centre of mass trails the Earth's orbit (via 3 slightly inclined orbits around the sun). Lasers, emitting from each SC to the other two, form six null connections and allow tracking of the inter-SC distances. Each connection (two per SC) entails a test mass (TM) within a gravitational reference system (GRS), an interferometric detection system (IDS) that includes an optical bench (OB), a telescope and a laser. The proper distance between TMs (shielded within each SC) is then measured by combining TM to OB and OB to OB interferometry data.

The TM, a 46mm cube of 2kg gold-platinum, and its surrounding hardware is known as the GRS. It is a house of electrodes with capacitive sensing to read the TM position with respect to the housing; this also enables electrostatic shielding of the TM and the use of nano-Newton forces to align the TM for optical measurement. It has a launch-lock device to protect the TM during launch and later release it. A UV illumination system can neutralise the TM from accumulation of static charges, while the vacuum chamber around the TM is maintained via a venting duct to space; the SC also houses gravitational balance masses required to compensate the self-gravity of the SC and instrumentation.

The telescopes both transmit and receive collimated beams between the neighbouring SC and their OBs; separation of the beams is ensured via different polarisations. Each OB consists of 3 interferometers: the inter-satellite interferometer tracks the relative motion (includes angular) between the OBs on each SC, the TM interferometer measures motion between the OB and the TM (again including angular), and the reference interferometer tracks relative phase fluctuations between the two lasers on board (one in each IDS); this measures differential laser frequency noise, which needs to be subtracted from the data streams. Each laser outputs a power of 2W, yet only a few 100 picowatts are received due to the dispersion of the beams travelling between SC. On reception, the incoming beam is beat against a local oscillator beam (where the dominating shot noise arises).

The telescope, laser and charge management system (minimises residual charge on TMs) are being developed by NASA with all other components being produced by ESA and its member states. We are currently in phase B2; the prime contractor has been selected (OHB), payload preliminary design review is in progress, and payload critical design review will begin shortly. The mission at this phase (implementation) has four structures: the instrument and project team, that is the ESA LISA Project, Performance and Operations Teams with all instrument providers; the science ground segment (SGS) (European Distributed Data Processing Centre, NASA SGS and Science Operations Centre); the LISA Science Team (LST) and its working groups; and the scientific community (including the LISA Consortium) that interacts with both the SGS and the LST. Details of the mission setup are in the Science Management Plan (SMP) [2].

3. LISA Science

The LISA science objectives are described in the LISA Redbook [1]; we focus on those tied to particular waveform models. In-depth reviews of the modelling and astrophysics can be found in the LISA Waveform and Astrophysics White Papers [3, 4] respectively.

3.1. **SO1: Study the formation and evolution of compact binary stars and the structure of the Milky Way Galaxy.** This mostly refers to double white dwarfs (DWDs), of which about 10^4 will be individually detectable by LISA; in turn, several hundred of these are expected to have electromagnetic (EM) counterparts enabling multi-messenger studies [5]. Ten's of EM signals have already been identified as DWDs detectable by LISA, the so-called verification binaries [6], which will assist in the scientific verification of the LISA data. It is expected that many more ($\sim 10^7$) DWDs will also emit in the LISA range building a stochastic Galactic foreground. Binaries consisting of either or both neutron stars (NSs) and black holes (BHs) should also be detectable from within our galaxy, however at much lower numbers (tens to hundreds).

In modelling, one only considers the inspiral as these binaries are at large separations and will not merge in the LISA band; thus the post-Newtonian (PN) approximation [7] is employed. In fact, due to weak GW emission at this stage, most signals are expected to be quasi-monochromatic (small frequency drift). A mass-transfer phase can occur in LISA-band DWDs, which determines the binary's fate: either a merger or stable mass transfer that counteracts GW radiation and widens the binary. Tidal effects are also important; their interplay with both mass transfer and GW emission is poorly understood and can affect the binary's final state [8]. For systems with NSs/BHs, close binaries inform us of their initial kick velocity from the individual NS/BH formation during supernova (already seen by EM observations for NSs); high kick velocities will tend to disrupt binaries and this will be observed in their distribution [9]. Indeed, the sheer number of expected detections will not only allow us to make statistical reasoning on all the above but also enables us to map out the Milky Way mass distribution as well as inform merger rates.

3.2. **SO2: Trace the origins, growth and merger histories of massive Black Holes across cosmic epochs.** Massive BH binaries (MBHBs: masses $\sim 10^6 - 10^9 M_\odot$) , are well outside the scope of ground detectors. LISA will see MBHBs out to arbitrarily large redshift as well as less massive binaries involving intermediate mass BHs (IMBHs: masses $\sim 10^2 - 10^5 M_\odot$). Little is known about IMBHs; only a few on the extremes of their mass range have ever been detected [10, 11, 12], allowing little insight into their origin and evolution spanning these masses. LISA's ability to detect them will spurn a new pool of knowledge. Meanwhile massive BHs (MBHs) have long been confirmed in both the present and early universe by EM observations, including accreting $10^6 M_\odot$ MBHs at redshifts $4 < z < 10$ [13, 14]. LISA's sensitivity to $10^3 - 10^7 M_\odot$ binaries at such redshifts will inform theories on BH growth and their host galaxies across the cosmos, in particular IMBHs at the epoch of MBH formation $z > 10$, which is outside all current telescope's abilities. This in turn will not only unveil insights into their origin, population and growth of mass but information on spin and merging rates. As the signals can stay in the detector from days to weeks (mass dependent), one can alert the global network of EM telescopes to search for multi-messenger signals. This could lead to environmental information on accretion as well as a wealth of complementary data (the only GW-EM multi-messenger to-date, GW170817, led to a groundbreaking number of scientific observations [15]).

In detecting MBHBs, a problem arises: LISA's sensitivity allows jarring SNRs (1000s), exasperating the infamous global fit problem. She will see all sources from all directions simultaneously (modulated by LISA's orbital motion); one must systematically identify and remove signals from the data. SNRs ~ 1000 require waveforms of unparalleled accuracy for removal without remnants poisoning lower-SNR signals. Comparable-mass binary models used by current ground detectors [16] combine PN and numerical relativity (NR), balancing speed, accuracy and parameter space coverage, e.g. effective one body [17, 18], phenomenological [19, 20] and NR surrogates [21]. Neither their current accuracy nor parameter space coverage is good enough for LISA MBHBs [3].

3.3. **SO3 Probe the properties and immediate environments of Black Holes in the local Universe using extreme mass-ratio inspirals and intermediate mass-ratio inspirals.** Compact objects are predicted to orbit and merge with MBHBs and IMBHs. Stellar-mass BHs ($5 - 10^2 M_\odot$) inspiralling into a MBHB, known as extreme mass-ratio inspirals (EMRIs), are expected to occur in galaxy centres. A stellar-mass BH merging with an IMBH or an IMBH with a MBHB, both called intermediate mass-ratio inspirals (IMRIs), are known as light or heavy respectively; light IMRIs are likely to arise in dense star clusters and dwarf galaxies. EMRIs and IMRIs both generate many GW cycles ($\sim 10^5$) in LISA's band, enabling tight constraints on the primary's spin ($\sim 10^{-5}$) as well as the secondary's eccentricity and inclination, while masses will be measured ($\sim 10^{-2}$). These constitute detections of MBHs and IMBHs accordingly and so will provide insights on the population, parameters and growth mechanisms. Inclination, eccentricity and spin will inform formation channels [22, 23, 24] while the environment (accretion disk [25], multiple bodies [26]) may also imprint on the waveforms.

In modelling EMRIs and IMRIs, PN struggles as the binary tightens, while NR slows for differing body sizes. The self-force (SF) program, which perturbs in the mass-ratio, has emerged as the primary modelling approach. The first post-adiabatic SF inspiral-only waveform [27] showed consistency with NR for mass-ratios as low as 10, affirming its application to IMRIs as well as EMRIs. Current models cover only circular inspirals, with a spinning secondary [28] and small primary spin ($\chi < 0.1$) [29], with promising merger-ringdown developments [30, 31]. Generic (spinning, eccentric, inclined) post-adiabatic SF waveforms are required for parameter estimation of EMRIs and IMRIs [32]; fast (less accurate) adiabatic waveforms for spinning eccentric systems have been developed in the meantime [33] for use in astrophysical studies and for data analysis developments. Combining NR with SF [34] or PN with SF fluxes [35] may also yield generic waveforms.

3.4. **SO4 Understand the astrophysics of stellar-mass Black Holes.** Over 200 stellar-mass BHBs (sBHBs) have been detected by the LIGO-Virgo-KAGRA collaboration (LVK) of ground detectors [36], which is expected to reach $\sim 10^4$ by the time LISA flies. These catch binaries merging, when most have circularised; LISA will see sBHBs earlier in their inspiral with sensitivity to eccentricity (informs formation channels) and possibly environmental effects. BHs that grew together, from massive stars of a stellar binary collapsing, expect low eccentricity and aligned spins. Binaries formed via dynamical capture will generate a more random distribution of spins in eccentric orbits. LISA may also detect higher-mass sBHBs, like GW190521 [37], that sit in the theoretical BH pair-instability mass-gap (a range of masses for which BHs can not form directly from star collapse [38]). BHs in this range form via hierarchal mergers [39] or a combination of mergers and accretion within a disk [40, 41], with each having their own signatures in the wavefroms [42], and hence environmental information. In addition LISA may see a sBHB that is later detected by ground detectors, allowing a multi-band detection and the ability to send early alerts (months prior to merger), with sky position and expected merger time (down to seconds), to both the EM community (to search for EM counterparts) and the ground detectors (ensure they are live). Multiband detections are notable probes in testing Einstein's relativity [43] and as dark sirens in cosmology [44], the subject of the fifth and sixth science objectives respectively (MBHBs and EMRIs also play large parts in these objectives but this is outside of the scope of this review). In modelling sBHBs, due to their comparable mass, one may use the same waveform families and techniques as MBHBs (where generic waveforms are also required).

4. The LISA Science Team (LST)

The LST, 20 scientists covering several expertise from institutes across Europe and USA, were selected over three calls. As per the SMP [2], the initial 18, announced in July 2024, included 6 from a NASA call, 11 from an ESA call and the LISA Consortium representative, in areas of Astrophysics (Neil Cornish, Erin Kara, Valeriya Korol, Astrid Lamberts, Gijs Nelemans, Elena Maria Rossi, Alberto Sesana, Joey Shapiro Key, Krista Lynne Smith, Alberto Vecchio), Cosmology (Chiara Caprini), Data Analysis (Nikolaos Karnesis, Antoine Petiteau, Stephen Taylor), Instrumentation (Guido Müller, William Joseph Weber) and Waveforms (Anna Heffernan, Deirdre Shoemaker). These were later joined in April 2025 by 2 ESA-selected complementary scientists in Space Weather (Catia Grimani) and Multi-Messenger (Zoltan Haiman), while in October 2025, transfer of the Consortium representative from Gijs Nelemans to Jonathan Gair began. The LST goals [2] are towards maximising the science return of LISA, including communications and access. Occasionally, an urgent matter leads to a taskforce formation; this was the case for LISA input into the European Strategy for Particle Physics, where a team (including external members) delivered a report within weeks due to a pressing deadline [45]. More defined longterm goals are tackled via working groups (WGs), which can invite external members. There are currently 6 WGs: Alerts, Author List, Communications, Figures of Merit (FoM), L3 Catalog and Science Topical Panels (STPs).

4.1. **The Alerts Working Group.** Set up at the LST face-to-face in December 2025, this WG is chaired by ZH and VK. The goals are to provide inputs and specifications to the DDPC for developing a pipeline for issuing alerts; design recommendations for SOC on when and how to operate this pipeline and issue alerts; and connect with communities outside LISA to ensure awareness and lead-time needed for triggered EM observations.

4.2. **The Author List Working Group.** This WG, chaired by NC, JG and GN, aims to create a set of criteria as well as a procedure to populate the heritage and member author lists as described in the SMP [2]. The heritage author lists those who have made a significant contribution to the mission and has no expiration data. The member author list comprises people working on the mission at the time of science operations and has a roll-off period of 2 years. To-date, a survey has been done among the LST members and information has been collected on criteria used by other missions / instruments for authorship. Descriptions of the member and heritage author lists have been formulated and discussed with the full LST. Based on this feedback, the description of the heritage list has been organized under the two categories, *Founders* and *Builders*. Next steps will be to create drafts of the criteria for membership and the selection procedure.

4.3. **The Communications Working Group.** The Comms WG, chaired by AH and KLS, aims to ensure smooth communications, both internal and external, formally and informally (via mutual members). Internal connects the different WGs, LST members, and project scientists. External refers to interested entities, including the Distributed Data Processing Centre (DDPC members: JG), NASA Science Ground Segment (NSGS: external member Ann Hornschemeier Cardiff of NASA), Lisa Consortium (AH, JG, VK, JSK), Gravitational Wave International Committee (GWIC: JG, AH, JSK) and other such stakeholders. Several lines of external communication have been established: the LST has an official email (LISAScienceTeam@esa.int), moderated by AH and KLS; a FAQ list has been created, which will go live on the ESA LISA website shortly (with other prepared material); close ties to the Consortium communications is set up via shared members VK and JSK; and living slides have been created for use by LST members to minimise repetitive work and unify messaging when presenting on LISA and LST. Internal links are being supported by streamlining interactions between the various WGs in reporting and presenting their progress and deliverables to both other LST members and the scientific community; this includes a response to questions document that ensures consistent messaging about mission timelines, outcomes, authorship, etc.

4.4. **The Figures of Merit Working Group.** Chaired by AP and AS, with several LST and external members, this WG is concerned with the Figures of Merit (FoM), a set of metrics designed to quantify the mission's ability to meet its science goals, creating a direct link from instrument specs to science objectives. They provide a key tool for the Performance & Operations team, particularly during the development phase when technical or financial constraints may require modifications to the instrument design. The FoM enable such changes to be assessed in terms of their impact on the scientific return of the mission. They also allow consideration for points of failure during the mission and the scientific consequences. For this reason, ESA has commissioned the LST to define and implement the FoM. The group is currently reviewing the existing set of FoM, both a static [46] and interactive site [47], prepared during earlier stages of the mission definition by the LISA Consortium and streamlining these to a final (LST) version. Ultimately, the WG will deliver a FoM Tool for the Performance & Operations team, understanding how to best achieve this is also being considered by the WG.

4.5. **The L3 Catalogue Working Group.** This WG, chaired by AL and NK, has been charged with determining the content and format of the Level 3 science catalogue, which is required to include GW candidates with detection confidence, estimated astrophysical parameters, strain time series, and the residual L1 datastream with candidate sources removed. The WG is working on identifying functional priorities and design features for data visualisation to enable preliminary analysis and catalog cross-matching; these will lead into detailed descriptions of tools to be developed for interfacing with the data that will be provided with the data releases. The goal for easy accessibility for all scientists requires considerations of accessibility issues for scientists with no GW speciality.

4.6. **The Science Topical Panels Working Group.** The goal of the Science Topical Panels (STP) WG, chaired by EMR and ST, is to determine the nature of STPs during the Early Release Science Time of the LISA mission, defined as approximately the first 12 months of data collection after a 3-month period of in-orbit commissioning [2]. The STP WG discusses potential panel topics, team composition (including chairs), required expertise, member responsibilities, interaction with the LISA Collaboration and the LISA Consortium, and how all of these issues feed into the solicitation and timeline procedure for topics and members. The goal of the WG is to generate a reduced set of proposed actions that encapsulate different scenarios for broader LST discussion. The STP WG has produced and presented a draft document to the LST that describes several possible procedures which lead to the formation of STPs. Further streamlining of this document, taking into consideration feedback from the LST, is in progress. In addition, an avenue for receiving feedback from the scientific community is being developed.

5. Acknowledgements

AH would like to thank her fellow members and project scientists of the LISA science team for their invaluable feedback and illuminating discussions, in particular, Neil Cornish, Jonathan Gair, Zoltan Haiman, Valeriya Korol, Nora Lützgendorf, Guido Müller, Gijs Nelemans, Krista Lynne Smith, Elena Maria Rossi and Joey Shapiro Key. This short review was partially completed while the author was visiting the Institute for Mathematical Sciences, National University of Singapore in 2025. AH is supported by grant PD-034-2023 co-financed by the Govern Balear and the European Social Fund Plus (ESF+) 2021-2027. This work was supported by the Universitat de les Illes Balears (UIB); the Spanish Agencia Estatal de Investigación grants PID2022-138626NB-I00, RED2024-153978-E, RED2024-153735-E, funded by MICIU/AEI/10.13039/501100011033 and the ERDF/EU; and the Comunitat Autònoma de les Illes Balears through the Conselleria d'Educació i Universitats with funds from the European Union - NextGenerationEU/PRTR-C17.I1 (SINCO2022/6719) and from the European Union - European Regional Development Fund (ERDF) (SINCO2022/18146).

References

[1] M. Colpi *et al.* LISA Definition Study Report. arXiv:2402.07571(2024).

[2] LISA Science Management Plan https://www.cosmos.esa.int/documents/15452792/15452811/LISA-Science-Management-Plan.pdf/ (2024)

[3] N. Afshordi *et al.* [LISA Consortium Waveform Working Group], Waveform Modelling for the Laser Interferometer Space Antenna. *Living Rev Rel.*, **28**, 9 (2025), arXiv:2311.01300.

[4] P. A. Seoane *et al.* [LISA Consoritum Astrophysics Working Group], Astrophysics with the Laser Interferometer Space Antenna. *Living Rev. Rel.* **26**, no.1, 2 (2023), arXiv:2203.06016.

[5] K. Breivik *et al.* Characterizing Accreting Double White Dwarf Binaries with the Laser Interferometer Space Antenna and Gaia,. *Astrophys. J. Lett.* **854**, no.1, L1 (2018), arXiv:1710.08370

[6] T. Kupfer *et al.* LISA Galactic Binaries with Astrometry from Gaia DR3. *Astrophys. J* **963**, no.2, 100 (2024), arXiv:2302.12719

[7] L. Blanchet, Post-Newtonian Theory for Gravitational Waves. *Living Rev. Rel.* **17**, 2 (2014), arXiv:1310.1528.

[8] T. R. Marsh, G. Nelemans and D. Steeghs, Mass transfer between double white dwarfs. *Mon. Not. Roy. Astron. Soc.* **350**, 113 (2004), arXiv:astro-ph/0312577.

[9] N. Giacobbo and M. Mapelli, The progenitors of compact-object binaries: impact of metallicity, common envelope and natal kicks. *Mon. Not. Roy. Astron. Soc.* **480**, no.2, 2011-2030 (2018), arXiv:1806.00001.

[10] A. G. Abac *et al.* [LIGO Scientific, VIRGO and KAGRA], GW231123: A Binary Black Hole Merger with Total Mass 190–265 $M_{\odot}$. *Astrophys. J. Lett.* **993**, no.1, L25 (2025), arXiv:2507.08219.

[11] D. Lin *et al.* A luminous X-ray outburst from an intermediate-mass black hole in an off-centre star cluster, *Nature Astron.* **2** (2018) no.8, 656-661 arXiv:1806.05692.

[12] J. E. Greene, J. Strader, L. C. Ho, Intermediate-Mass Black Holes, *Annu. Rev. Astron. Astrophys.* **58** (2020), 257-312 arXiv:1911.09678.

[13] R. Maiolino *et al.* JADES - The diverse population of infant black holes at $4 < z < 11$: Merging, tiny, poor, but mighty, *Astron. Astrophys.* **691** (2024), A145 arXiv:2308.01230.

[14] R. Maiolino *et al.* A small and vigorous black hole in the early Universe, *Nature* **627** (2024) no.8002, 59-63 [erratum: Nature **630** (2024) no.8015, E2] arXiv:2305.12492.

[15] B. P. Abbott *et al.* Multi-messenger Observations of a Binary Neutron Star Merger, *Astrophys. J. Lett.* **848** (2017) no.2, L12 arXiv:1710.05833.

[16] A. G. Abac *et al.* [LIGO Scientific, VIRGO and KAGRA], GWTC-4.0: Methods for Identifying and Characterizing Gravitational-wave Transients, arXiv:2508.18081.

[17] A. Ramos-Buades, A. Buonanno, H. Estellés, M. Khalil, D. P. Mihaylov, S. Ossokine, L. Pompili and M. Shiferaw, Next generation of accurate and efficient multipolar precessing-spin effective-one-body waveforms for binary black holes, *Phys. Rev. D* **108** (2023) no.12, 124037 arXiv:2303.18046.

[18] S. Akcay *et al.* Effective-one-body multipolar waveform for tidally interacting binary neutron stars up to merger, *Phys. Rev. D* **99** (2019) no.4, 044051 arXiv:1812.02744.

[19] M. Colleoni *et al.* Fast frequency-domain gravitational waveforms for precessing binaries with a new twist, *Phys. Rev. D* **111** (2025) no.10, 104019 arXiv:2412.16721.

[20] J. E. Thompson, E. Hamilton, L. London, S. Ghosh, P. Kolitsidou, C. Hoy and M. Hannam, PhenomXO4a: a phenomenological gravitational-wave model for precessing black-hole binaries with higher multipoles and asymmetries, *Phys. Rev. D* **109** (2024) no.6, 063012 arXiv:2312.10025.

[21] V. Varma *et al.* Surrogate models for precessing binary black hole simulations with unequal masses, *Phys. Rev. Research.* **1** (2019), 033015 arXiv:1905.09300.

[22] C. Hopman and T. Alexander, The Orbital statistics of stellar inspiral and relaxation near a massive black hole: Characterizing gravitational wave sources, *Astrophys. J.* **629** (2005), 362-372 arXiv:astro-ph/0503672.

[23] M. Coleman Miller, M. Freitag, D. P. Hamilton and V. M. Lauburg, Binary encounters with supermassive black holes: Zero-eccentricity LISA events, *Astrophys. J. Lett.* **631** (2005), L117-L120 arXiv:astro-ph/0507133.

[24] M. Volonteri, P. Madau, E. Quataert and M. J. Rees, The Distribution and cosmic evolution of massive black hole spins, *Astrophys. J.* **620** (2005), 69-77 arXiv:astro-ph/0410342.

[25] F. Duque, L. Sberna, A. Spiers and R. Vicente, Extreme-mass-ratio inspirals in relativistic accretion discs, arXiv:2510.02433.

[26] Z. Pan, H. Yang, L. Bernard and B. Bonga, Resonant dynamics of extreme mass-ratio inspirals in a perturbed Kerr spacetime, *Phys. Rev. D* **108** (2023) no.10, 104026 arXiv:2306.06576.

[27] B. Wardell *et al.* Gravitational Waveforms for Compact Binaries from Second-Order Self-Force Theory, *Phys. Rev. Lett.* **130** (2023) no.24, 241402 arXiv:2112.12265.

[28] J. Mathews, A. Pound and B. Wardell, Self-force calculations with a spinning secondary, *Phys. Rev. D* **105** (2022) no.8, 084031 arXiv:2112.13069.

[29] J. Mathews, B. Wardell, A. Pound and N. Warburton, Post-adiabatic self-force waveforms: slowly spinning primary and precessing secondary, arXiv:2510.16113.

[30] L. Küchler, G. Compère and A. Pound, Self-force framework for merger-ringdown waveforms, arXiv:2506.02189.

[31] L. Honet, L. Küchler, A. Pound and G. Compère, Transition-to-plunge self-force waveforms with a spinning primary, arXiv:2510.13958.

[32] O. Burke *et al.* Assessing the importance of first postadiabatic terms for small-mass-ratio binaries, *Phys. Rev. D* **109** (2024) no.12, 124048 arXiv:2310.08927.

[33] C. E. A. Chapman-Bird *et al.* Efficient waveforms for asymmetric-mass eccentric equatorial inspirals into rapidly spinning black holes, *Phys. Rev. D* **112** (2025) no.10, 104023 arXiv:2506.09470.

[34] N. A. Wittek, L. Barack, H. P. Pfeiffer, A. Pound, N. Deppe, L. E. Kidder, A. Macedo, K. C. Nelli, W. Throwe and N. L. Vu, Relieving Scale Disparity in Binary Black Hole Simulations, *Phys. Rev. Lett.* **134** (2025) no.25, 251402 arXiv:2410.22290.

[35] L. Honet *et al.* Spin-aligned inspiral waveforms from self-force and post-Newtonian theory, arXiv:2510.16112.

[36] A. G. Abac *et al.* [LIGO Scientific, VIRGO and KAGRA], GWTC-4.0: Population Properties of Merging Compact Binaries, arXiv:2508.18083.

[37] R. Abbott *et al.* [LIGO Scientific and Virgo], GW190521: A Binary Black Hole Merger with a Total Mass of $150M_{\odot}$, *Phys. Rev. Lett.* **125** (2020) no.10, 101102 arXiv:2009.01075.

[38] S. E. Woosley and A. Heger, The Pair-Instability Mass Gap for Black Holes, *Astrophys. J. Lett.* **912** (2021) no.2, L31 arXiv:2103.07933.

[39] D. Gerosa and M. Fishbach, Hierarchical mergers of stellar-mass black holes and their gravitational-wave signatures, *Nature Astron.* **5** (2021) no.8, 749-760 arXiv:2105.03439.

[40] H. Tagawa, B. Kocsis, Z. Haiman, I. Bartos, K. Omukai and J. Samsing, Mass-gap Mergers in Active Galactic Nuclei, *Astrophys. J.* **908** (2021) no.2, 194 arXiv:2012.00011.

[41] I. Bartos and Z. Haiman, Accretion is All You Need: Black Hole Spin Alignment in Merger GW231123 Indicates Accretion Pathway, *Astrophys. J. Lett.* **996** (2026) no.2, L44 arXiv:2508.08558.

[42] K. Inayoshi, N. Tamanini, C. Caprini and Z. Haiman, Probing stellar binary black hole formation in galactic nuclei via the imprint of their center of mass acceleration on their gravitational wave signal, *Phys. Rev. D* **96** (2017) no.6, 063014 arXiv:1702.06529

[43] T. Baker, E. Barausse, A. Chen, C. de Rham, M. Pieroni and G. Tasinato, Testing gravitational wave propagation with multiband detections, *JCAP* **03** (2023), 044 arXiv:2209.14398

[44] N. Muttoni, A. Mangiagli, A. Sesana, D. Laghi, W. Del Pozzo, D. Izquierdo-Villalba and M. Rosati, Multiband gravitational wave cosmology with stellar origin black hole binaries, *Phys. Rev. D* **105** (2022) no.4, 043509 arXiv:2109.13934

[45] C. Caprini *et al.* [LISA Science Team], Science of the LISA mission: A Summary for the European Strategy for Particle Physics, arXiv:2507.05130 (2025)

[46] LISA Consortium Figures of Merit (Static), https://wiki-lisa.in2p3.fr/fom-sites/dc_82_fmin_1e-4/site/ (2024)

[47] LISA Consortium Figures of Merit (Interactive), https://lisa-science-explorer.in2p3.fr/ (2024)

Departament de Física, Universitat de les Illes Balears, IAC3 – IEEC, Crta. Valldemossa km 7.5, E-07122 Palma, Spain

Email address: anna.heffernan@uib.eu

PUTTING THE HYPE IN HYPERBOLIC BLACK HOLE SCATTERING

OLIVER LONG

Classification AMS 2020:

Keywords: General Relativity, Gravitational waves, Black hole scattering, Numerical Relativity, Self-force, Post-Minkowskian, Effective One Body

This talk summarises recent advances in the modelling of hyperbolic black hole scattering, a scenario of increasing interest for the gravitational wave community. While these scattering encounters have not been observed with current detectors [1, 2], multiple works have suggested that they may be observed with future detectors [3, 4]. Furthermore, scattering encounters provide a useful theoretical laboratory for testing and comparing different approaches to the two-body problem in General Relativity. The talk will highlight the key findings from recent studies in post-Minkowskian, self-force, Numerical Relativity, and Effective One Body theory, and their implications for our understanding of black hole dynamics.

Post-Minkowskian (PM) theory is a weak-field approximation where the spacetime is expanded order-by-order in Newton's constant G. PM calculations have seen significant progress in recent years due to the adaptation of advanced techniques from particle physics to the two-body problem. The state-of-the-art calculations have now reached the 5th order in G up to linear order in the mass ratio [5].

Self-force (SF) theory is an alternative expansion in the mass ratio of the two bodies, which is valid at all separations if the mass ratio is sufficiently small. While SF on bound orbits have been extensively studied, the case of unbound orbits has been restricted to a scalar field toy model in order to develop the necessary computational infrastructure [6]. These calculations have been compared to PM results showing good agreement in the weak-field regime [7]. SF information has also been used to improve the accuracy of PM results in the strong-field regime by incorporating information about the scatter-capture separatrix. This resummation has been shown to significantly improve the accuracy of PM results across all separations [8].

In order to study strong-field interactions in the comparable mass regime we must use Numerical Relativity (NR) where the full Einstein equations are solved on a computer. While progress in NR was fueled by the need to model late-inspiral and merger of quasi-circular binaries, recent works have simulated hyperbolic black hole encounters. These simulations have been used to extract the scattering angle with recent results being the first to extend the simulations up to mass ratios of 1:10 and measure disparate scattering angles of each black hole due to assymetric gravitational wave emission [9].

Finally, the Effective One Body (EOB) formalism provides a framework to model the two-body problem across all mass ratios and separations by mapping it to an effective one-body problem. Recent work compared different models of hyperbolic scattering within the EOB framework to NR results, finding that the most recent EOB models show very good agreement with NR across a range of mass ratios and impact parameters [9].

This comparison has also highlighted areas where further improvements can be made, particularly in the case of spinning black holes where so-called “evolution” models show large discrepancies with NR results [9].

References

[1] G. Morrás, J. García-Bellido, and S. Nesseris, “Search for black hole hyperbolic encounters with gravitational wave detectors,” *Phys. Dark Univ.* **35**, 100932 (2022),

[2] S. Bini, S. Tiwari, Y. Xu, L. Smith, M. Ebersold, G. Principe, M. Haney, P. Jetzer, and G. A. Prodi, “Search for hyperbolic encounters of compact objects in the third LIGO–Virgo–KAGRA observing run,” *Phys. Rev. D* **109**, 042009 (2024),

[3] J. García-Bellido and S. Nesseris, “Gravitational wave energy emission and detection rates of Primordial Black Hole hyperbolic encounters,” *Phys. Dark Univ.* **21**, 61–69 (2018)

[4] S. Mukherjee, S. Mitra, and S. Chatterjee, “Gravitational wave observatories may be able to detect hyperbolic encounters of black holes,” *Mon. Not. Roy. Astron. Soc.* **508**, 5064–5073 (2021).

[5] M. Driesse, G. U. Jakobsen, A. Klemm, G. Mogull, C. Nega, J. Plefka, B. Sauer, and J. Usovitsch, “Emergence of Calabi–Yau manifolds in high-precision black-hole scattering,” *Nature* **641**, 603–607 (2025).

[6] L. Barack and O. Long, “Self-force correction to the deflection angle in black-hole scattering: A scalar charge toy model,” *Phys. Rev. D* **106**, 104031 (2022).

[7] L. Barack *et al.*, “Comparison of post-Minkowskian and self-force expansions: Scattering in a scalar charge toy model,” *Phys. Rev. D* **108**, 024025 (2023).

[8] O. Long, C. Whittall, and L. Barack, “Black hole scattering near the transition to plunge: Self-force and resummation of post-Minkowskian theory,” *Phys. Rev. D* **110**, 044039 (2024).

[9] O. Long, H. P. Pfeiffer, A. Buonanno, G. U. Jakobsen, G. Mogull, A. Ramos-Buades, H. R. Rüter, L. E. Kidder, and M. A. Scheel, “Highly accurate simulations of asymmetric black-hole scattering and cross validation of effective-one-body models,” arXiv:2507.08071 [gr-qc] (2025).

Email address: `oliver.long@aei.mpg.de`

Max Planck Institute for Gravitational Physics (Albert Einstein Institute), D-14476 Potsdam, Germany

THE DDPC AND EMRI WAVEFORM MODELLING: STRUCTURE, ROLES, AND ROADMAP

PHILIP LYNCH

Classification AMS 2020:

Keywords: Gravitational waves, black holes, waveform modelling, extreme mass ratio inspirals

1. Introduction

The European Space Agency's (ESA) Laser Interferometer Space Antenna (LISA) is a space-based gravitational-wave observatory scheduled for launch in 2035. The Distributed Data Processing Centre (DDPC) is one of two primary ground segments in the LISA mission, responsible for transforming raw telemetry data (level 0) into a scientifically validated catalogue of gravitational-wave sources (level 3). The DDPC provides the full analysis chain from instrument calibration to the production of a final catalogue, functioning alongside ESA's Science Operations Centre (SOC). An independent pipeline run by the NASA Science Ground Segment (NSGS). The DDPC is comprised of a set of Coordination Units (CUs), each addressing a distinct stage of the data-processing pipeline or providing support to the pipeline's development and testing. This paper outlines the DDPC structure, the function of each CU, and the roadmap for the Waveform Coordination Unit (CU Wav), with emphasis on the Extreme Mass Ratio Inspiral (EMRI) subunit.

2. DDPC Structure and Coordination Units

The DDPC comprises multiple CUs aligned with successive data-processing levels and key operational domains:

- **CU L01 (Level 0 - Level 1):** Converts raw spacecraft telemetry into time-delay interferometry (TDI) channels.Tasks include data cleaning, instrument calibration, and laser-noise suppression via TDI combinations, and the development of the L0-L1 pipeline, 'Lolipops'.
- **CU L2A (Alerts):** Implements low-latency source detection and preliminary parameter estimation, and provides alerts for multi-messenger astronomy.
- **CU L2D (Deep):** Develops and hosts the Global Fit Pipeline which uses Bayesian inference for joint analysis of all detectable sources. The current focus is on massive black hole binaries (MBHBs) and galactic binaries (GBs), with planned inclusion of EMRIs, stellar-origin black-hole binaries, stochastic backgrounds, and non-astrophysical artifacts such as glitches and data gaps.
- **CU L3C (Catalogue):** Builds the final catalogue of sources, selecting the most relevant parameters and metadata for community dissemination.

- **CU SIM (Simulations):** Generates synthetic datasets for validation. This includes both instrument noise and mock populations of gravitational-wave sources. They produce the LISA Data Challenges, providing controlled environments to test pipelines and models.
- **CU Wav (Waveforms):** Manages waveform model quality assurance via waveform reviews, defines waveform conventions, and develops a Waveform Generator.

Each CU operates semi-autonomously but is interlinked through shared interfaces and review procedures, ensuring that the pipeline components integrate smoothly with one another.

3. CU Wav

CU Wav is responsible for the verification and standardization of waveform models used across DDPC pipelines. Importantly, it is **not** responsible for the development of the waveform models themselves. Its central activities are:

(1) **Waveform Review Process:** An internal peer-review system assessing code quality, robustness, and compatiability with DDPC piplinees and hardware (rather than physical accuracy). Reviews include code inspection, compilation tests across platforms, pertubation tests, injection and recovery parameter estimation tests, and convention consistency checks.
(2) **Waveform Generator Development:** Creation of a standardized interface that allows all CUs to call waveform models in a uniform way. The generator currently supports Phenom and SEOB models for MBHBs, models for GBs, and models for the LISA instrument response, but will be extended to include more source types.
(3) **Conventions:** Establishing consistent parameter definitions and conventions across waveform models and providing conversions between conventions.

4. The EMRI Subunit

The EMRI subunit within CU Wav currently includes 14 members with expertise ranging from post-adiabatic (1PA) waveform modelling to EMRI search and parameter estimation. The group meets bi-weekly and coordinates through dedicated communication channels. Its primary goal is to establish the validation framework and deliver a roadmap for EMRI waveform readiness for the LISA data-analysis pipelines. The subunit's current focus is on vacuum General Relativity models within the FastEMRIWaveforms (FEW) framework [1]. Models from different frameworks can also be reviewed if they are to be utlised within the DDPC.

5. EMRI Waveform Review Programme

The subunit has defined a staged review plan:

(1) **Eccentric Kerr Adiabatic Model (0PA)** [2]**:** first waveform review for an EMRI waveform model, starting September 2025.
(2) **1PA Quasi-Circular Model with Spin** [3]**:** review scheduled for mid-2026.
(3) **Spherical (Circular and Inclined) 0PA Model:** requires the inclusion of polar modes and improved interpolation; review planned for late 2026.

(4) **Generic (Eccentric + Inclined) 0PA Model:** development of efficient 4D interpolation methods; review targeted for 2027.

Parallel efforts include implementing secondary-spin effects, orbital resonances, and hybrid approaches combining gravitational self-force (GSF) and post-Newtonian (PN) inputs. These developments aim to support a fully realistic EMRI waveform model in time for the LISA Critical Design Review (CDR) in 2032, including spinning secondaries and resonant dynamics.

6. Timeline and Milestones

The EMRI subunit roadmap aligns with the overall DDPC schedule:

- 2025–2026: Establish waveform-review protocols, finalize Waveform Generator specifications, and validate early EMRI models (Eccentric Kerr 0PA, 1PA Circular).
- 2026–2028: Expand reviews to spherical and generic waveform models, consolidate waveform conventions.
- 2029–2030: Deliver a validated, efficient EMRI waveform models compatible with the Global Fit pipeline, in time for catalogue generation before the LISA Critical Design Review (CDR 2032).

Intermediate milestones include integration into the Mojito (2026) and Long Island Iced Tea (2030) data challenges (2025–2027).

7. Outlook and Community Involvement

LISA's success in detecting and characterizing EMRIs depends on community-driven model development. The DDPC provides the framework, but the broader research community must contribute by:

- Developing FEW or developing alternative frameworks.
- Producing robust, well-documented, and efficient codes that can tile parameter space with GSF information.
- Advancing 2nd order GSF and PN-based hybrid models.
- Implementing secondary-spin and resonance effects.
- Exploring beyond-GR or environmental effects that can be modeled within the two-timescale adiabatic framework.

Collaborators are encouraged to engage early so models can be reviewed and integrated within the DDPC schedule.

References

[1] Michael L Katz et al. Fast extreme-mass-ratio-inspiral waveforms: New tools for millihertz gravitational-wave data analysis. *Phys. Rev. D*, 104 6, 064047, 2021.

[2] Christian E. A. Chapman-Bird et al. The Fast and the Frame-Dragging: Efficient waveforms for asymmetric-mass eccentric equatorial inspirals into rapidly-spinning black holes *arXiv*, 2506.09470, 2025.

[3] Ollie Burke et al. Assessing the importance of first postadiabatic terms for small-mass-ratio binaries. *Phys. Rev. D*, 109 12, 124048, 2024.

Max Planck Institute for Gravitational Physics (Albert Einstein Institute), Am Mühlenberg 1, 14476 Potsdam, Germany

Email address: philip.lynch@aei.mpg.de

The Hyperboloidal Framework in the gravitational self-force programme

Rodrigo Panosso Macedo

Center of Gravity, Niels Bohr Institute, Blegdamsvej 17, 2100 Copenhagen, Denmark

rodrigo.macedo@nbi.ku.dk

Overview

The hyperboloidal framework has emerged as a powerful geometric and numerical approach for treating wave propagation on black-hole backgrounds [1–5]. Its central idea—rooted in Penrose's conformal treatment of infinity [6]—is to combine a conformal mapping of the spacetime [7–9] and foliate the conformal manifold with spacelike hypersurfaces that asymptote to future null infinity while remaining regular across black-hole horizons. This construction enables the simultaneous resolution of near-horizon and asymptotic regions within a single coordinate patch and eliminates the need for artificial outer boundaries, thereby avoiding spurious reflections and boundary-condition systematic errors.

Hyperboloidal methods play an increasingly important role in the modelling of gravitational radiation from black-hole systems, especially in regimes requiring extreme accuracy or controlled asymptotics. For perturbative approaches, including first- and second-order metric perturbations and gravitational self-force computations, the hyperboloidal formulation offers an attractive alternative to standard choices of coordinates based on Boyer–Lindquist or Schwarzschild slicing. It provides a unified description of both the black-hole exterior region (up to the event horizon) and the radiation zone (extending to $\mathscr{I}^+$), with all relevant geometric structures incorporated directly at the level of the differential equations.

Perturbation theory and the role of hyperboloidal slicing. Schematically, Einstein's equations take the form

$$\Box_g \Phi = S + \mathcal{N}(\Phi, \partial\Phi), \tag{1}$$

for a given field Φ representing some combination of metric or curvature components. This form emphasises the wave-equation character dictating the dynamics. Nonlinear couplings between Φ and its lower-order derivatives are captured by $\mathcal{N}$, whereas S represents possible sources. For the two-body problem in the extreme-mass-ratio regime, S assumes the form of distributional sources (e.g. a point particle) within the gravitational self-force programme [10].

Given the small parameter $\epsilon = m/M \ll 1$ naturally arising in extreme-mass-ratio inspirals, one can solve eq. (1) perturbatively by expanding the metric as

$$g = g_o + \epsilon g^{(1)} + \epsilon^2 g^{(2)} + \cdots \tag{2}$$

In the linear regime, the primary task is to solve

$$\Box_{g_o} \Phi^{(1)} = S^{(1)},$$

with g_o a stationary black-hole metric. At higher order, the source terms depend on the lower-order solutions; any systematic error in the first-order calculation therefore propagates and may jeopardise the second-order problem. This makes control of asymptotic behaviour and boundary regularity essential.

Hyperboloidal coordinates provide this control: the principal part of the transformed wave operator becomes singular at both the event horizon and $\mathscr{I}^+$, and the physically relevant ingoing/outgoing boundary conditions become directly encoded as regularity conditions. In particular, the radiative degree of freedom can be extracted unambiguously at null infinity without the need for extrapolation. Ref. [2] gives a detailed and updated review of the fundamentals of this research programme.

Self-force calculations. At first order, the gravitational self-force programme requires solving the linearised field equations with a distributional worldline source. These equations are solved either in the time or frequency domain. Exploring symmetries of the background spacetime, one typically projects the equations into a harmonic basis [11], decomposing the problem into a set of equations for individual (ℓ, m)-modes characterising the angular structure of the field. This strategy leads to $(1{+}1)D$ wave equations in the time domain, or $1D$ ordinary differential equations in the frequency domain. Recently, there has been interest in treating the equations within an m-mode strategy [12, 13], thereby avoiding the decoupling between the radial and polar angular directions. In all the above-mentioned strategies, regularisation schemes are required to obtain physical observables at the particle's position [10].

Over the past years, the hyperboloidal framework has been consistently adapted to the needs of first-order calculations within the gravitational self-force programme. Initial efforts concentrated on toy models given by a scalar field on the Schwarzschild background, with a particle in a circular orbit. In this context, successful results have been demonstrated in the time domain [14–16] and in the frequency domain [13, 17].

Currently, the research programme aims to include scenarios of increasing relevance to gravitational-wave physics. The challenges include: (i) extension of the framework beyond scalar-field toy models into the gravitational case; (ii) considering the Kerr solution for the background metric; and (iii) modelling the particle's trajectory in more intricate orbits. Ref. [18] made significant progress in tackling step (i) for circular orbits in the Schwarzschild background, by solving the first-order metric perturbation in the Lorenz gauge within the hyperboloidal framework. For step (ii), the infrastructure put forward in ref. [13] was developed with a direct extension to Kerr in mind, and work in this direction is in progress. Finally, step (iii) constitutes one of the major challenges. In this context, the next section introduces initial ideas for treating the problem of particles on eccentric equatorial orbits.

Elliptic-coordinate mapping for future m-mode PDE solvers

For eccentric-orbit self-force calculations, the particle librates between radial turning points σ_- and σ_+. A promising strategy for improving spectral resolution in the near-particle region is to introduce an *elliptic coordinate mapping* adapted to this libration domain. The idea is to reinterpret the physical hyperboloidal coordinates (σ, y) in an excision region around the particle's trajectory in terms of shifted elliptical coordinates (μ, ν) centred at the midpoint of the libration interval.

Construction of the map. Standard planar elliptic coordinates are defined by

$$x = a\cosh\mu\cos\nu, \qquad y = a\sinh\mu\sin\nu,$$

with $\mu \in [0, \mu_0]$ and $\nu \in [0, \pi]$. The parameter μ_0 fixes the size of the excision region and world tube around the particle.

To adapt this map to the physical hyperboloidal coordinates, we shift the x coordinate to be centred at the midpoint of the libration region σ_0, and we place the focal points at the turning points $\sigma_\pm$, by imposing $\sigma_\pm - \sigma_0 = \pm a$.

This strategy leads to the physical coordinate map

$$\sigma = \frac{\sigma_+ + \sigma_-}{2} + \frac{\sigma_+ - \sigma_-}{2}\cosh\mu\,\cos\nu, \quad y = \frac{\sigma_+ - \sigma_-}{2}\sinh\mu\,\sin\nu, \tag{3}$$

which naturally parametrises grid points near the particle worldline in a similar way to the polar coordinate map used for circular orbits (see fig. 1). Its introduction into future hyperboloidal m-mode solvers provides a potential geometrical strategy and may help bridge time-domain and frequency-domain approaches within a unified framework. A possible enhancement may require adjusting the elliptic coordinates to a system adapted to the particle's co-moving frame [12, 13].

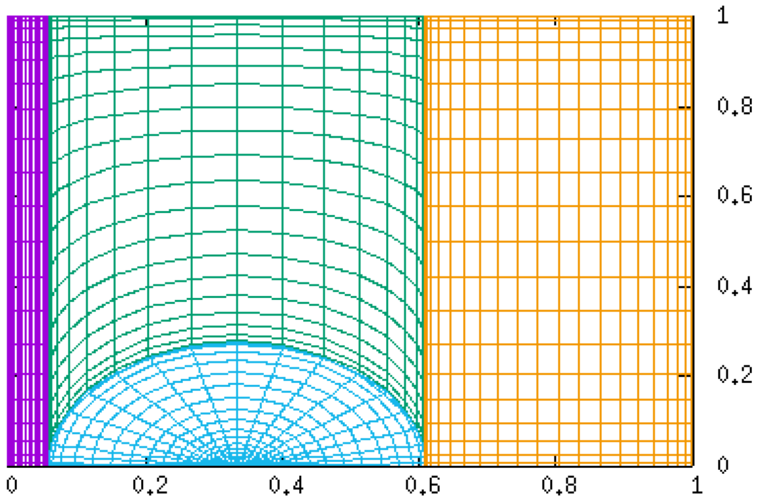

FIGURE 1. Elliptic coordinates mapped into hyperboloidal (σ, y) coordinates as a potential geometrical strategy for an m-mode solver for an eccentric equatorial orbit.

CONCLUDING REMARKS

The hyperboloidal framework, together with modern spectral solvers and geometric domain decompositions, offers a promising path toward next-generation self-force calculations. The incorporation of elliptic-coordinate mappings represents a natural and flexible extension of the method, potentially enabling accurate and efficient solutions of the m-mode elliptic PDEs associated with eccentric inspirals. This line of development is particularly timely given the demands of future space-based detectors such as *LISA*, where controlled asymptotics, high-accuracy mode extraction, and robust treatment of distributional sources will be indispensable.

Acknowledgement

I would like to thank the hospitality and financial support by the Institute for Mathematical Sciences, National University of Singapore. I also acknowledge support by VILLUM Foundation (grant no. VIL37766) and the DNRF Chair program (grant no. DNRF162) by the Danish National Research Foundation. The Center of Gravity is a Center of Excellence funded by the Danish National Research Foundation under grant No. 184.

References

[1] Anil Zenginoglu. A Geometric framework for black hole perturbations. *Phys. Rev. D*, 83:127502, 2011.

[2] Rodrigo Panosso Macedo. Hyperboloidal approach for static spherically symmetric spacetimes: a didactical introductionand applications in black-hole physics. *Phil. Trans. Roy. Soc. Lond. A*, 382(2267):20230046, 2024.

[3] Rodrigo Panosso Macedo and Anil Zenginoglu. Hyperboloidal approach to quasinormal modes. *Front. in Phys.*, 12:1497601, 2024.

[4] Emanuele Berti et al. Black hole spectroscopy: from theory to experiment. *arXiv 2505.23895*, 2025.

[5] David Hilditch, Rodrigo Panosso Macedo, Alex Vañó-Viñuales, and Anıl Zenginoğlu. Topical Collection-Hyperboloidal Foliations in the Era of Gravitational-Wave Astronomy: From Mathematical Relativity to Astrophysics. *Gen. Rel. Grav.*, 57:131, 2025.

[6] Roger Penrose. Republication of: Conformal treatment of infinity. *General Relativity and Gravitation*, 43(3):901–922, 2011. Originally published in 1964; reprinted in the Golden Oldies series.

[7] Jorg Frauendiener. Conformal infinity. *Living Rev. Rel.*, 3:4, 2000.

[8] J. Frauendiener and H. Friedrich, editors. *The conformal structure of space-time: Geometry, analysis, numerics*, 2002.

[9] Juan A. Valiente Kroon. *Conformal Methods in General Relativity*. Oxford University Press, 2017.

[10] Leor Barack and Adam Pound. Self-force and radiation reaction in general relativity. *Rept. Prog. Phys.*, 82(1):016904, 2019.

[11] Adam Pound and Barry Wardell. Black hole perturbation theory and gravitational self-force. 1 2021.

[12] Patrick Bourg, Adam Pound, Samuel D. Upton, and Rodrigo Panosso Macedo. Simple, efficient method of calculating the Detweiler-Whiting singular field to very high order. *Phys. Rev. D*, 110(8):084007, 2024.

[13] Rodrigo Panosso Macedo, Patrick Bourg, Adam Pound, and Samuel D. Upton. Multidomain spectral method for self-force calculations. *Phys. Rev. D*, 110(8):084008, 2024.

[14] Lidia J. Gomes Da Silva, Rodrigo Panosso Macedo, Jonathan E. Thompson, Juan A. Valiente Kroon, Leanne Durkan, and Oliver Long. Hyperboloidal discontinuous time-symmetric numerical algorithm with higher order jumps for gravitational self-force computations in the time domain. *arXiv 2306.13153*, 2023.

[15] Lidia J. Gomes Da Silva. DiscoTEX 1.0: Discontinuous collocation and implicit-turned-explicit (IMTEX) integration symplectic, symmetric numerical algorithms with higher order jumps for differential equations I: numerical black hole perturbation theory applications. *arXiv 2401.08758*, 2024.

[16] Lidia J. Gomes Da Silva. DiscoTEX 1.0: Discontinuous collocation and implicit-turned-explicit (IMTEX) integration symplectic, symmetric numerical algorithms with high order jumps for differential equations II: extension to higher-orders of numerical convergence. *arXiv 2411.14399*, 2024.

[17] Rodrigo Panosso Macedo, Benjamin Leather, Niels Warburton, Barry Wardell, and Anıl Zenginoğlu. Hyperboloidal method for frequency-domain self-force calculations. *Phys. Rev. D*, 105(10):104033, 2022.

[18] Benjamin Leather. Gravitational self-force with hyperboloidal slicing and spectral methods. *Gen. Rel. Grav.*, 57(7):112, 2025.

COMPUTATIONAL ADVANCES IN SELF-FORCE: BUILDING A BRIDGE BETWEEN THEORY AND WAVEFORM MODELING

ZACHARY NASIPAK

Classification AMS 2020: 83C35, 83C25

Keywords: perturbation theory, gravitational waves, multiscale expansions

1. Background

The multiscale self-force (MSF) framework provides an efficient and systematic method for modeling compact binaries with disparate masses and their associated gravitational-wave signals [5]. In this framework, the binary's mass ratio $\epsilon = m_2/m_1$ is treated as a perturbative parameter, and the full spacetime metric $\mathrm{g}_{\mu\nu}$ is decomposed as

$$\mathrm{g}_{\mu\nu} = g_{\mu\nu} + h_{\mu\nu}, \qquad h_{\mu\nu} = \epsilon h^{(1)}_{\mu\nu} + \epsilon^2 h^{(2)}_{\mu\nu} + \cdots , \tag{1.1}$$

where $g_{\mu\nu}$ is the background metric of the larger mass m_1 and $h_{\mu\nu}$ encodes the perturbations sourced by the smaller body m_2. Due to the gradual inspiral of disparate mass systems and their quasi-periodic nature, these perturbations are further decomposed into "fast" oscillating phases $\phi_a \doteq (\phi_r, \phi_\theta, \phi_\phi)$ and "slowly"-evolving orbital phase-space variables J_b (e.g., energy, angular momentum, frequencies),

$$h^{(n)}_{\mu\nu} = \sum_{k^a} h^{(n)k^a}_{\mu\nu}(J) e^{-ik^a\phi_a}, \tag{1.2}$$

where $k^a \doteq (k_r, k_\theta, k_\phi)$. The amplitudes $h^{(n)k^a}_{\mu\nu}(J)$ are parametrized purely by J_b, and once computed across this space, they determine the inspiral dynamics, fast phase evolution, and resulting gravitational-wave signals order by order in ϵ.

At leading-order in this multiscale expansion, the system undergoes adiabatic radiation-reaction in which time-averaged gravitational wave fluxes [which can be computed from the asymptotic amplitudes of $h^{(1)k^a}_{\mu\nu}(J)$] drive the secular decay of the binary orbit over the inspiral timescale $T_{\mathrm{insp}} \sim M/\epsilon$. These leading-order dynamics—often referred to as adiabatic or 0-post-adiabatic (0PA) order—contribute $O(\epsilon^{-1})$ cycles to the gravitational wave signal. At subleading or 1PA order, conservative corrections from $h^{(1)}_{\mu\nu}$ and dissipation driven by $h^{(2)}_{\mu\nu}$ contribute $O(1)$ cycles to the gravitational wave phase. MSF waveform models must therefore include both 0PA and 1PA contributions in order to achieve the subradian phase accuracy required to meet the science goals of both ground- and space-based observatories.

2. Results

Current MSF waveform models incorporating 0PA and 1PA effects have successfully described the inspiral of black hole binaries with mass ratios as comparable as $\epsilon \sim 0.1$ [6]. However, these models, and the associated precomputed 0PA and 1PA data, remain restricted to non-spinning black holes on quasi-circular orbits. Recent work has extended the framework to eccentric binaries with spin, but only at the 0PA level, leaving the 1PA data required for subradian accuracy still unavailable [1]. A central challenge lies in the computationally intensive offline stage in which the amplitudes of $h^{(1)}_{\mu\nu}$ and $h^{(2)}_{\mu\nu}$ must be computed across a large region of parameter space. This precomputed database then serves as the essential input for the subsequent rapid online generation of waveforms. Extending these 0PA and 1PA datasets to more realistic eccentric, spinning, and precessing systems is an interesting theoretical challenge and crucial for the next generation of gravitational-wave astronomy.

In this talk, I outline how recent computational advances are bridging the gap between the theoretical foundations of the MSF framework and the practical generation of 0PA and 1PA data products for accurate MSF waveform models. I review which specific information from $h^{(1)}_{\mu\nu}$ and $h^{(2)}_{\mu\nu}$ needs to be computed and stored across the parameter space, with a particular focus on

- 0PA fluxes, computed from the asymptotic amplitudes of $h^{(1)}_{\mu\nu}$, with a focus on the results of Refs. [1, 2];
- 1PA redshift corrections $\langle z_1 \rangle$, computed from the local behavior of $h^{(1)}_{\mu\nu}$ along the worldline of m_2, with a focus on the results of Refs. [3]; and
- 1PA dissipative corrections, which are derived from the asymptotic amplitudes of $h^{(2)}_{\mu\nu}$, with a focus on the results of Refs. [6].

I highlight recent progress in computing these quantities, enabled in part by the development of open-source tools such as the MATHEMATICA packages in the Black Hole Perturbation Toolkit [7] and the PYTHON library `pybhpt` [3, 4]. These resources are making it increasingly feasible to extend 0PA and 1PA data into new regions of parameter space, as evidenced by the recent work of Refs. [1, 3]. I also discuss ongoing advances in constructing second-order perturbations in Kerr spacetime—an essential milestone for producing subradian (1PA-accurate) waveforms for binaries with spinning and precessing black holes.

REFERENCES

1. Christian E. A. Chapman-Bird et al., *The Fast and the Frame-Dragging: Efficient waveforms for asymmetric-mass eccentric equatorial inspirals into rapidly-spinning black holes*, (2025).
2. Scott A. Hughes, Niels Warburton, Gaurav Khanna, Alvin J. K. Chua, and Michael L. Katz, *Adiabatic waveforms for extreme mass-ratio inspirals via multivoice decomposition in time and frequency*, Phys. Rev. D **103** (2021), no. 10, 104014, [Erratum: Phys.Rev.D 107, 089901 (2023)].
3. Zachary Nasipak, *Metric reconstruction and the Hamiltonian for eccentric, precessing binaries in the small-mass-ratio limit*, (2025).
4. Zachary Nasipak, *znasipak/pybhpt: v0.9.5*, September 2025.
5. Adam Pound and Barry Wardell, *Black hole perturbation theory and gravitational self-force*, (2021).
6. Barry Wardell, Adam Pound, Niels Warburton, Jeremy Miller, Leanne Durkan, and Alexandre Le Tiec, *Gravitational Waveforms for Compact Binaries from Second-Order Self-Force Theory*, Phys. Rev. Lett. **130** (2023), no. 24, 241402.
7. Barry Wardell, Niels Warburton, Kevin Cunningham, Leanne Durkan, Benjamin Leather, Zachary Nasipak, Chris Kavanagh, Adrian Ottewill, Marc Casals, Theo Torres, Jakob Neef, and Susanna Barsanti, *Teukolsky*, June 2025.

Email address: `z.nasipak@soton.ac.uk`

SECOND-ORDER SELF-FORCE: STATE OF PLAY

ADAM POUND

It is well understood that to achieve target accuracy for LISA, EMRI models must be carried to first post-adiabatic order (1PA) in a multiscale expansion. This requires solving at least part of the Einstein field equations at second perturbative order in the binary's mass ratio. Over the past 15 years, significant progress has been made in overcoming conceptual and technical challenges in this endeavour, leading to the production of a 1PA waveform model for nonspinning, quasicircular binaries in 2021. More recently, theoretical advances have been made to resolve errors in that model, and further progress has been made in extending them to the realistic case of a spinning, Kerr primary. In this talk I summarize the current state of play.

UNIVERSITY OF SOUTHAMPTON, UK
Email address: `a.pound@soton.ac.uk`

FIX THE FRAME, RESOLVE THE MEMORY: THE BONDI–SACHS GAUGE IN BLACK HOLE PERTURBATION THEORY

ANDREW SPIERS

Keywords: Black hole perturbation theory, Bondi–Sachs gauge, BMS symmetries, gravitational wave memory, second-order self-force

Understanding gauge and frame dependence is crucial for extracting physical observables from black hole perturbation theory (BHPT) [1], especially as calculations extend to second-perturbative order. At second order, constructing gauge-invariant quantities is challenging. Quantities that are gauge-invariant at linear order become gauge-dependent when extended to second order. The gauge dependence of second-order calculations introduces scope for working in poorly behaved gauges, which produce singular source terms. Near future null infinity generic gauges produce singular sources (so-called infrared divergences) such that integrals do not converge [4].

Further subtleties arise in the gauge choice of second-order calculation near future null infinity. Gravitational-wave memory is frame-dependent and will be detectable with next-generation detectors such as LISA [**?**]. When measuring gravitational waveforms or comparing waveforms between models, not including the memory effect consistently can cause errors. Gravitational memory effects are associated with choices of gauge near future null infinity; working in consistent gauges between models, and the frame of gravitational detectors, allows one to consistently incorporate gravitational memory effects [6].

To address these challenges, we construct a perturbative treatment of the Bondi–Sachs (BS) gauge on Kerr spacetime, accompanied by a BMS frame-fixing scheme. The BS gauge enforces the canonical Bondi–Sachs falloff and determinant conditions on the metric near future null infinity, ensuring that the retarded-time foliation and luminosity distance are uniquely defined. Our formalism allows one to transform to the BS gauge with a prescribed BMS frame from any initial gauge at first order. The BMS frame corresponds to a choice of supertranslation and Lorentz frame that fixes the residual asymptotic freedom of the BS gauge, thereby providing an unambiguous notion of angular coordinates and Bondi time. Our method provides a consistent way to extract memory effects associated with the BMS frame. Additionally, the BS gauge avoids infrared divergences, and using our first-order gauge fixing scheme, we define second-order gauge invariants near future null infinity.

Our derivation begins with the Kerr metric expressed in BS coordinates, following the prescription in Bai et al. [2]. The Kerr BS coordinates are defined using an asymptotic expansion in terms of Boyer–Lindquist coordinates. Hence, these Kerr BS coordinates are only exactly in BS form at future null infinity; within the interior, they are only approximately in BS form in the large radius limit. Nonetheless, this approximate BS structure suffices for our analysis, and the asymptotic expansion can be extended as required.

We define the *perturbative BS gauge* by specifying gauge conditions on the first-order metric perturbation. The transformation to this gauge is described by a vector field satisfying a hierarchical set of first-order ODEs along outgoing null rays, with boundary conditions applied at future null infinity satisfying the BS gauge. Introducing an asymptotic expansion of the metric perturbation reduces these equations to an algebraic form. For practical implementation, we recast the gauge vector in Boyer–Lindquist coordinates and decompose it into Newman–Penrose components.

Residual freedom in the perturbative BS gauge corresponds to the BMS frame. We analyse this freedom in our perturbative BS gauge and give a BMS frame fixing scheme based on choices for the Bondi mass aspect and the Wald–Zoupas angular momentum aspect on a given retarded time-slice at future null infinity. Our procedure constrains the supertranslation, boosts, and rotation degrees of freedom, leaving only the background Killing symmetries (time translations and axial rotations), which can be fixed by waveform alignment. The resulting prescription fully determines the integration constants in our perturbative BS gauge transformation vector calculation.

Although our explicit construction is developed at first order, we leverage it to define second-order gauge-invariant quantities near null infinity. We use the second-order Weyl scalars

$$\{\psi_{4L}^{(2)},\ \psi_4^{(2)},\ \psi_{0L}^{(2)},\ \psi_0^{(2)}\}$$

are invariant under purely second-order gauge vector transformations [7, 8]. By fixing the first-order gauge with our perturbative BS formalism, these scalars become genuine gauge invariants (invariant under first- and second-order gauge transformations) between asymptotically flat gauges. Hence, applying our BS gauge vector calculation allows one to construct second-order gauge invariants associated to the BS gauge using gauge fixing.

Implementing our BS gauge fixing scheme has further advantages for second-order calculations. Re-expressing the second-order Teukolsky equation [7, 8] in a gauge-fixed form, associated with an asymptotically flat gauge (such as the perturbative BS gauge), naturally avoids infrared divergences and provides a consistent framework to extract gravitational-wave memory. Our methods will be used to help compute second-order self-force calculations in Schwarzschild and Kerr spacetime and enable systematic comparisons between second-order results and other approaches, including post-Newtonian and post-Minkowskian theory, ringdown calculations, and numerical relativity.

References

[1] S. Chandrasekhar. ”The Mathematical Theory of Black Holes” Vol. 69. Oxford university press, 1998

[2] S. Bai, et al. Light cone structure near null infinity of the Kerr metric. Physical Review D—Particles, Fields, Gravitation, and Cosmology 75.4 (2007): 044003.

[3] B. Wardell et al. Gravitational Waveforms for Compact Binaries from Second-Order Self-Force Theory Physical Review Letters 130.24 (2023): 241402.

[4] K. Cunningham, et al. Gravitational memory: new results from post-Newtonian and self-force theory. Classical and Quantum Gravity 42.13 (2025): 135009.

[5] Favata, Marc. The gravitational-wave memory effect. Classical and Quantum Gravity 27.8 (2010): 084036.
[6] Mitman, Keefe, et al. A review of gravitational memory and BMS frame fixing in numerical relativity. Classical and Quantum Gravity 41.22 (2024): 223001.
[7] Campanelli, Manuela, and Carlos O. Lousto. Second order gauge invariant gravitational perturbations of a Kerr black hole. Physical Review D 59.12 (1999): 124022.
[8] Spiers, Andrew, Adam Pound, and Jordan Moxon. Second-order Teukolsky formalism in Kerr spacetime: Formulation and nonlinear source. Physical Review D 108.6 (2023): 064002.

SCHOOL OF MATHEMATICAL SCIENCES, UNIVERSITY OF NOTTINGHAM, UK
Email address: andrew.spiers@nottingham.ac.uk

MEMORY AND HYBRIDIZATION FOR CONNECTING THE NUMERICAL AND ANALYTICAL TWO-BODY PROBLEM

LEO STEIN

We need numerical solutions to the relativistic two-body problem where analytical methods break down: the late inspiral, merger, and onset of ringdown. I will first give a brief overview of the third numerical relativity waveform catalog from the SXS collaboration. But numerics have their own limitations, so to create a complete solution we need to combine numerical and analytical information into a ”hybrid” solution. The process of hybridizing creates its own challenges: What gauges are we using? How do numerical and analytical parameters map onto each other? I will detail some challenges arising in hybridization, including the importance of gravitational memory and BMS frames.

THE UNIVERSITY OF MISSISSIPPI, USA
Email address: `lcstein@olemiss.edu`

INTEGRABILITY OF THE RELATIVISTIC TWO-BODY PROBLEM

VOJTĚCH WITZANY

Classification AMS 2020: 83C10, 83C57, 83C35, 70H06, 70H08, 70H40, 70H33, 37J06, 37J35, 37J40

Keywords: General relativity, Black holes, Neutron stars, Gravitational waves, Compact objects, Binary inspirals, Equations of motion, Integrability, KAM theory, Multiple scale perturbation methods

The relativistic two-body problem is central to gravitational wave astrophysics, particularly for modeling compact binary inspirals and the resulting gravitational-wave signals. It represents one of the simplest dynamical problems in general relativity, yet it is significantly more complex than its Newtonian counterpart due to the inherent length scale set by the gravitational radius and the presence of spin and radiation-reaction effects. This abstract summarizes a presentation on the integrability of such systems under various approximations, emphasizing the role of symmetries, perturbations, and dissipative effects.

We begin with a review of *Hamiltonian integrable dynamics*, where a system with N degrees of freedom is Liouville integrable if there exist N functionally independent, commuting constants of motion. According to the Liouville-Arnold theorem [1], the motion is confined to invariant tori and can be solved by quadratures. In action-angle coordinates $(\mathbf{J}, \boldsymbol{\theta})$, the Hamiltonian becomes $H(\mathbf{J})$, and the equations of motion simplify to:

$$\dot{\boldsymbol{\theta}} = \frac{\partial H}{\partial \mathbf{J}} \equiv \boldsymbol{\Omega}, \quad \dot{\mathbf{J}} = 0. \tag{0.1}$$

The *Kolmogorov-Arnold-Moser (KAM) theorem* ensures that most invariant tori survive under small perturbations of size ϵ. However, tori satisfying a local resonance condition $\boldsymbol{\Omega} \cdot \boldsymbol{k} = 0$, where $\boldsymbol{k}$ is an integer vector, may be destroyed and replaced by nonlinear oscillations of amplitude $\sim \sqrt{\epsilon}$. Between the surviving tori and the resonant oscillations, a thin chaotic layer generically emerges. Although the resonance condition is fulfilled on a dense set in phase space, only resonant tori with small $\boldsymbol{k}$ vectors are practically relevant. This is because the amplitude of the resonant oscillations scales with the size of the $\boldsymbol{k}$-harmonic of the perturbation with respect to θ, which decays exponentially as $\sim e^{-C|\boldsymbol{k}|}$ for large $|\boldsymbol{k}|$. This allows for a practical cutoff in resonance analysis.

In conservative approximations of the relativistic two-body problem, integrability is preserved up to certain post-Newtonian (PN) orders. Systems of two point particles with only orbital degrees of freedom are integrable due to Poincaré symmetries, yielding six commuting integrals: energy, total linear momentum, one component of the total angular momentum, and its magnitude. However, the inclusion of spin introduces additional degrees of freedom and potential non-integrability. Known integrable cases include Kerr geodesics [2], spinning test particles [3, 4, 5], and spinning compact binaries at general mass ratios in certain PN regimes [6, 7].

Actions serve as coordinate-independent invariants that bridge PN and test-particle limits. These quantities depend only on the homotopy class of phase-space loops and are known to match across regimes [8]. However, integrability is fragile: tidal interactions, internal modes (e.g., f-modes in neutron stars), and environmental effects generically break it [9, 10].

For inspiraling binaries, we define integrability as the existence of a convergent two-timescale expansion up to the transition to plunge. The equations of motion can then be cast in action-angle variables, and near-identity transformations can be applied to eliminate angle dependence from the right-hand sides [1]:

$$\dot{\mathbf{J}} = \epsilon \mathbf{g}_1(\mathbf{J}) + \epsilon^2 \mathbf{g}_2(\mathbf{J}) + \dots, \tag{0.2}$$

$$\dot{\boldsymbol{\theta}} = \boldsymbol{\Omega}(\mathbf{J}) + \epsilon \mathbf{f}_1(\mathbf{J}) + \dots \tag{0.3}$$

Transient resonances from gravitational self-force (GSF) corrections can violate this structure [11]. In particular, resonant terms in the perturbation break the convergence of the near-identity expansion. A specific feature of the dissipative case is the dependence of the dissipation on the so-called resonant phase [12]. Resonances caused by other perturbative sources also disrupt the transformation, requiring alternative treatments.

The analysis reveals that switching between formulations of the equations of motion near resonances is necessary when $\boldsymbol{\Omega} \cdot \mathbf{k} \sim \epsilon^{\beta}$, with $\beta \in (0, 1/2)$ depending on the scheme [13, 14].

In conclusion, integrability persists in many regimes of the relativistic two-body problem but is not guaranteed. Understanding its limits is essential for accurate modeling of gravitational wave sources. Existing schemes can handle weak integrability breaking, but future work should focus on self-consistent evolution through resonances, gauge-invariant formulations, and a systematic mapping of resonant effects.

References

[1] Arnol'd, V. I., Kozlov, V. V., Neishtadt, A. I., & Iacob, I. (2006). *Mathematical Aspects of Classical and Celestial Mechanics* (Vol. 3). Springer, Encyclopaedia of Mathematical Sciences.

[2] Carter, B. (1968). Global structure of the Kerr family of gravitational fields. *Physical Review*, 174(5), 1559–1571.

[3] Rüdiger, R. (1981). Conserved quantities of spinning test particles in general relativity. I. *Proceedings of the Royal Society of London. A. Mathematical and Physical Sciences*, 375(1761), 185–193.

[4] Rüdiger, R. (1983). Conserved quantities of spinning test particles in general relativity. II. *Proceedings of the Royal Society of London. A. Mathematical and Physical Sciences*, 385(1788), 229–239.

[5] Witzany, V. (2019). Hamilton-Jacobi equation for spinning particles near black holes. *Physical Review D*, 100(10), 104030.

[6] Wu, X., & Xie, Y. (2010). Symplectic structure of post-Newtonian Hamiltonian for spinning compact binaries. *Physical Review D*, 81(8), 084045.

[7] Tanay, S., Stein, L. C., & Gálvez Ghersi, J. T. (2021). Integrability of eccentric, spinning black hole binaries up to second post-Newtonian order. *Physical Review D*, 103(6), 064066.

[8] Witzany, V., Skoupý, V., Stein, L. C., & Tanay, S. (2025). Actions of spinning compact binaries: Spinning particle in Kerr matched to dynamics at 1.5 post-Newtonian order. *Physical Review D*, 111(4), 044032.

[9] Steinhoff, J., Hinderer, T., Buonanno, A., & Taracchini, A. (2016). Dynamical Tides in General Relativity: Effective Action and Effective-One-Body Hamiltonian. *Physical Review D*, 94(10), 104028.

[10] Bonga, B., Yang, H., & Hughes, S. A. (2019). Tidal resonance in extreme mass-ratio inspirals. *Physical Review Letters*, 123(10), 101103.
[11] Flanagan, É. É., & Hinderer, T. (2012). Transient resonances in the inspirals of point particles into black holes. *Physical Review Letters*, 109(7), 071102.
[12] Flanagan, É. É, Hughes, S. A., & Ruangsri, U. (2014). Resonantly enhanced and diminished strong-field gravitational-wave fluxes. *Physical Review D*, 89(8), 084028.
[13] Lukes-Gerakopoulos, G., & Witzany, V. (2021). Nonlinear effects in EMRI dynamics and their imprints on gravitational waves. In *Handbook of Gravitational Wave Astronomy* (pp. 1–44). Springer, Singapore.
[14] Lynch, P., Witzany, V., van de Meent, M., & Warburton, N. (2024). Fast inspirals and the treatment of orbital resonances. *Classical and Quantum Gravity*, 41(22), 225002.

INSTITUTE OF THEORETICAL PHYSICS, CHARLES UNIVERSITY, PRAGUE, CZECH REPUBLIC
Email address: vojtech.witzany@matfyz.cuni.cz

PROBING FORMATION CHANNELS OF EXTREME MASS-RATIO INSPIRALS

HUAN YANG

Classification AMS 2020: 83C35

Keywords: Extreme Mass-ratio Inspiral, Active Galactic Nucleus

In this talk, I discuss how to probe formation channels and environmental effects of extreme mass-ratio inspirals (EMRIs), which are one of the main extragalactic sources of space-borne gravitational wave detectors. I have focused on two major channels - dry EMRIs that are produced through gravitational scatterings in nuclear star clusters and wet EMRIs that have Active Galactic Nucleus (AGN) playing a critical role to transport compact objects to the vicinity of massive black holes. The main content of this talk is based on our recent publications [1, 2, 3].

1. Direct measurement

The main astrophysical environmental effects of EMRIs may come from accretion disks, nearby stellar-mass objects, and/or dense dark matter distribution. On the one hand, these environmental objects may affect the gravitational waveform through the tidal resonance, as first discussed in [4, 5]. On the other hand, they may introduce additional dissipation channels, and also directly modify the total flux of the gravitational wave radiation during the secular evolution (as the background spacetime deviates from Kerr). We have been developing a general formalism to analyze the long-term secular motion of EMRIs in a perturbed black hole spacetime. Taking the scenario for a rotating black hole surrounded by a Axion cloud (as dark matter candidate), we manage to compute the extra scalar radiation due to the presence of the cloud [2]. In [3] we present the formalism to compute the modification of gravitational wave flux is the background deviates from Schwarzschild. The next step is to combine both effects due to scalar and (extra) gravitational wave radiation to obtain the EMRI waveform with these clouds, in order to allow future detections.

2. Indirect measurement

If the environmental effects, such as the disk effects are not directly observed in a set of EMRIs, we may still probe their population properties by studying the distribution of the key system parameters. With the population model developed in [1], we show the eccentricity of dry EMRIs are mostly (more than 99% percentile) larger than 0.01. The wet EMRIs, on the other hand, tend to have much smaller eccentricities because of disk dissipation, but they are not zero due to disk turbulence effects and multi-body mean-motion resonance in the disk. The turbulent eddies within a disk are generally associated with density fluctuations, so that they introduce fluctuating gravitational force on the EMRI object. The population model predicts that the resulting eccentricity should be mostly smaller than 0.01. In addition, the population model also predicts that a significant fraction of disks may host more than one stellar-mass object for $r \sim \mathcal{O}(10^2)$

gravitational radii. These object likely form mean-motion resonance pairs during their migration within the disk, and excite eccentricity to the level of $\mathcal{O}(10^{-4})$. As a result, eccentricity is a key observable to distinguish wet and dry formation channels. More importantly, it may be used to probe the level of turbulence within an AGN disk.

There are other observables that show distinct distribution in different EMRI formation channels, including the inclination angle, the mass, etc. In particular, the wet EMRI mass distribution is affected by EMRI capture probability onto the disk, the accretion process, and the chance of forming pairs and merge within the disk. The resulting mass distribution may show rich and different signatures compared with the mass distribution of black holes within LIGO-Virgo catalogs. So a precise measurement on the mass distribution may being valuable information on the evolution of stellar-mass black holes within AGN disks.

3. Summary

We have shown the properties of formation channels of EMRIs can be measured through both direct and indirect methods. In particular, the study in [1] represents the first step of probing formation mechanisms through population modelling. In the future, there are many unanswered questions and open discovery space for both directions.

References

[1] Houyi Sun, Ya-Ping Li, Zhen Pan, Huan Yang, Probing formation channels of extreme mass-ratio inspirals. *arXiv:* 2509.00469.

[2] Dongjun Li, Colin Weller, Patrick Bourg, Michael Lahaye, Nicolas Yunes, Huan Yang, Extreme mass-ration inspirals within an ultralight scalar cloud: Scalar radiation. *Phys. Rev. D*, 112, 084057, 2025.

[3] Michael Lahaye, Colin Weller, Dongjun Li, Patrick Bourg, Yanbei Chen, Huan Yang, Evolving extreme mass-ratio inspirals in a perturbed Schwarzschild spacetime. *arXiv:* 2510.16102.

[4] Huan Yang, Marc Casals, General relativistic dynamics of an extreme mass-ratio binary interacting with an external body. *Phys. Rev. D* 94, 083015, 2017.

[5] Beatrice Bonga, Huan Yang, Scott Hughes, Tidal Resonance in Extreme Mass-Ratio Inspirals. *Phys. Rev. Lett.* 123, 101103, 2019.

Department of Astronomy, Tsinghua University, Beijing 100084, China
Email address: hyangdoa@tsinghua.edu.cn